CHAPTER 3

ELECTRICITY GENERATION AND STORAGE WITH SEMICONDUCTOR SEPTUM SOLAR CELLS

3.1 INTRODUCTION

The semiconductor septum is the heart of SC-SEP solar cell. Cadmium chalcogenides such as CdSe, CdTe, CdS etc. are important materials as photoanodes for SC-SEP cells. Cadmium selenide (CdSe) has shown great promise as a semiconductor material for photoelectrochemical conversion because of its near ideal direct band gap (~ 1.7 eV). Several preparation techniques have been used to prepare large size polycrystalline thin films of CdSe for PEC applications. Here we have selected d.c. electrodeposition technique to deposit CdSe films.

In 1975, Gerischer [1] succeeded in the direct conversion of solar energy into electricity, a strategy that offers the possibility of both solar energy conversion and storage : PEC cells.

In the photoelectrolytic cell, the optical energy is converted into chemical energy. The photogenerated holes are used to oxidise one type of species and the electrons are used to reduce another type of species. Such a chemical species can be electrochemially discharged for the production of electricity. Such study on PEC cells and PEC storage cells have been appeared in the literature [2-15]. PEC cells have been used as rechargeable electrochemical storage cells, redox couple storage cells and septum cells.

A novel two-compartment solar cell, separated by semiconductor termed the semiconductor septum electrochemical photovoltaic (SC-SEP) cell and modeled after natural photosynthesis. It has been demonstrated by Tien [12] to generate hydrogen from seawater without externall applied voltage using only the visible light of solar spectrum. Semiconductor septum electrochemical photovoltaic cells consisting of two chambers, separated by a bipolar electrode made of either CdSe or $CdSe_xTe_{1-x}$ are reported by Ottova et al [13].

The solar energy storage with the help of semiconductor septum cells is reported by Pawar and Patil [15] using Fe_2O_3 semiconductor septum and different electrolytes. The photoelectrochemical redox storage cell using electrodeposited CdSe as semiconductor septum is reported by Pawar et al [16]. The solar to electrical load conversion efficiency of this cell is 4.06% for $CrCl_3$ electrolyte.

A single converter cell, solar to electrical, is called a solar cell or photovoltaic cell. The combination of such cells; designed to increase the electric power output is called a solar module. For practical applications, several such modules are mounted on a stack and connected with wire to form the final output. This final setup is called an array. For terrestial applications, silicon solar arrays have shown operating efficiencies of about 12 to 15%.

In the present investigation, we have studied preparation of large size n-CdSe films. An attempt has been made to store the solar energy in the form of chemical energy using n-CdSe semiconductor septum cells. The charging discharging cycles under illumination and dark respectively, has been carried out for different number of cells, for different area of semiconductor films and for different concentrations of $FeCl_3$ electrolyte in compartment II. We have studied series combination, parallel combination and series parallel combination as a modelling of n-CdSe semiconductor septum cells. Corrosion of septum cell due to $FeCl_3$ concentration has been also studied.

3.2 EXPERIMENTAL

3.2.1 Electrodeposition of Large Size CdSe Films

There are various methods for the deposition of thin films which are as follows :

Vapour deposition [17-19], chemical bath deposition [20], spray pyrolysis [21], pulse deposition [22], electrodeposition [23] etc. The choice of the particular method depends on the several factors like material to be deposited, nature of the substrate, required film thickness, structure of the film, application of the film, etc.

In recent years, electrodeposited thin film semiconductors are becoming popular in the fields of solar cells, optoelectronic devices, solar selective coating, etc. The preparation of thin film semiconductors with the electrodeposition technique has some advantages over other physical and chemical deposition techniques.

i. It is easy and economical, as semiconductors with no or small waste of materials could be prepared

ii. It is not required to have very pure starting materials

iii. The semiconductor properties like n-or p-type conductivity band-gap variation, control of stoichiometry, doping etc. could be controlled with a reasonable accuracy, as the parameters like deposition current and plating time can be controlled to be accuracy of μc and μs respectively [24-26]

iv. It is an isothermal process, mainly controlled by electrical parameters such as electrode voltage and current density, which are easily adjusted to control film thickness, morphology, composition etc.

v. Electrodeposition usually have low operating temperatures.

vi. It is particularly suited to the fabrication of heterojunction solar cells, simply by changing the deposition electrolyte, an n-type film can be deposited onto a p-type substrate.

Apart from single crystals, pressure sintered polycrystalline disc, Chandra and Pandey [27-29] have obtained CdSe films on metal substrates by electrodeposition from an acidic solution containing $CdSO_4$ and SeO_2. Lokhande et al. [30] have prepared CdSe thin films, using cathodic electrodeposition technique in alkaline and acidic baths. Thin films of $cdSe_x Te_{1-x}$ have been prepared on SnO_2 and Ti substrates by Murali et al. [31] using cathodic electrodeposition technique.

The electrodepositon cell is shown in Figure 3.1. It consists of,

(a) Cylindrical croning glass container having 14 cm in length and 11 cm in diameter, containing electrolyte.

(b) Backelite holder consisting two slots, one for substrate, second for counter electrode and one hole for saturated calomal electrode (SCE), with attachment of screws to hold them.

The films of CdSe were electrodeposited onto stainless steel substrate from a bath containing 10 mM $CdSO_4$ solution and 10 mM SeO_2 solution.. Both the solutions were

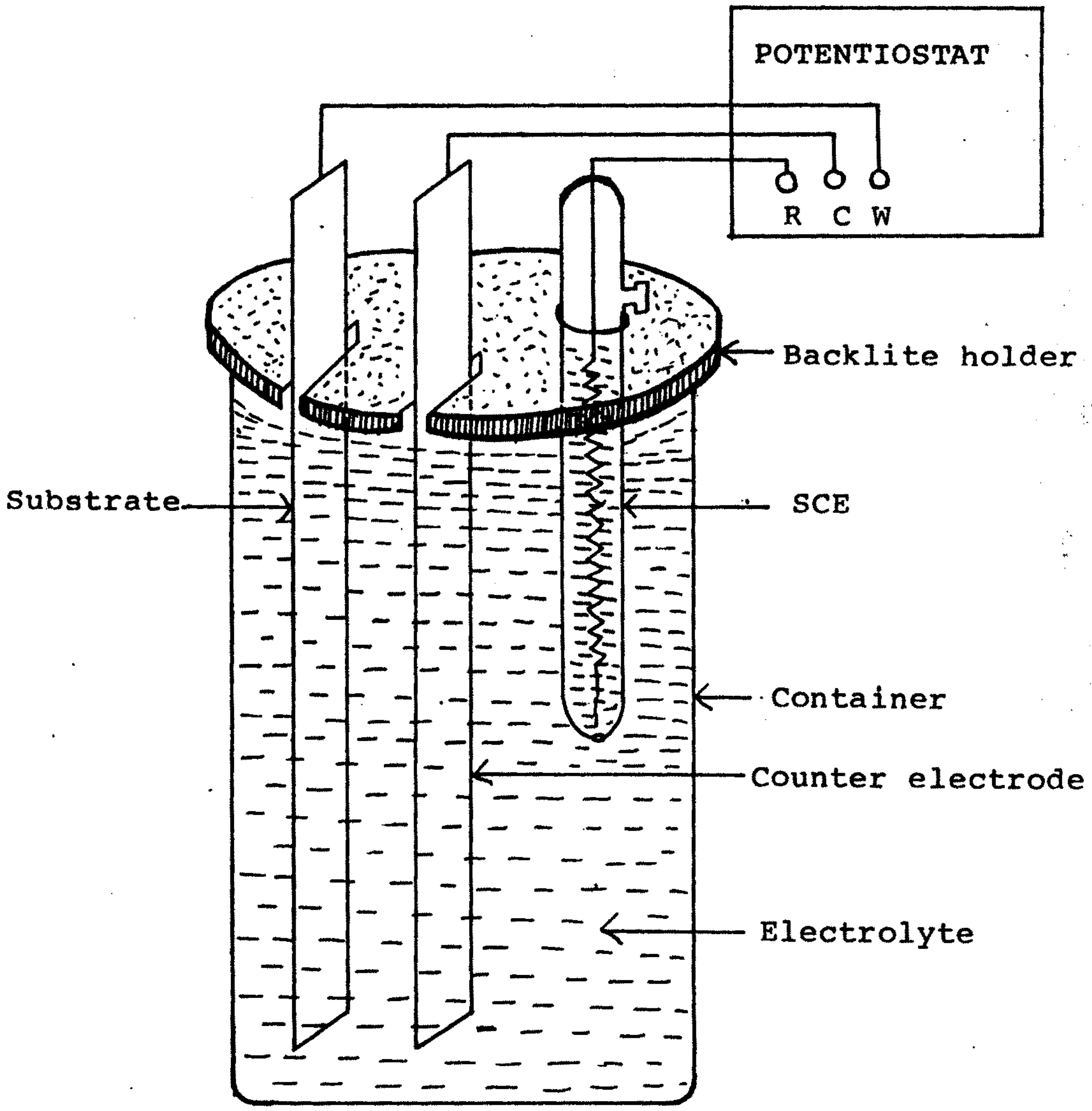

Fig.3.1. Schematic diagram of electrodeposition cell

prepared in double distilled water. The films were deposited under D.C. potentiostatic conditions using potentiostat model 362 (EG & G). Three electrode system was employed and the potential were measured with respect to saturated calomal electrode.

How this curve is made is not clear for the fig 3.2

The potential applied for deposition was -0.65 V (vs SCE), which was fixed from cathodic polarisation curve which is shown in Figure 3.2. pH of the solution was 2.9. The deposition time was 60 min. The back side of the stainless steel substrate was covered with insulating tape to avoid the back side deposition. The experimental set up is shown in Figure 3.3. The distance between counter electrode and substrate was 1 cm. Commercially available stainless steel (AISI-302 type) was used as substrate. The counter electrode was also same steel. The size of substrate and counter electrode was 9 X 14 cm^2.

CdSe films were prepared electrolytically on the basis of the principle adopted by Panicker et al. [32] by co-depositing Cd and Se on a conducting base such as steel. The electrolytic bath contained an aqueous solution of $3CdSO_4$, $8H_2O$ and SeO_2 powder. The CdSe thin film thus prepared.

Deposition of a thin film of CdSe is described as,

$$SeO_2 + H_2O \rightleftharpoons H_2SeO_3 \qquad (1)$$

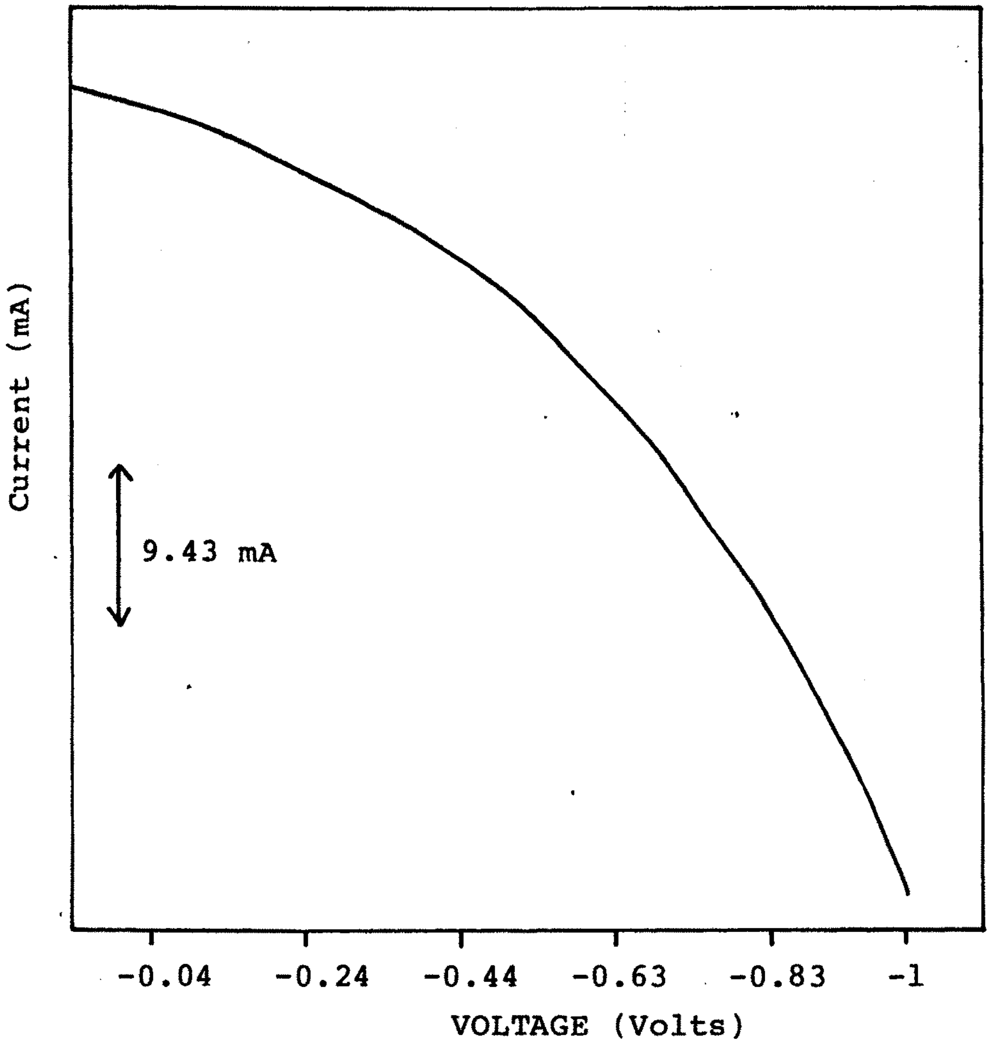

Fig.3.2. Cathode polarisation curve for CdSe deposition.

Fig.3.3. Experimental set-up for electrodeposition (photograph).

$$H_2SeO_3 + 4H^+ + 4e = Se + 3H_2O \qquad (2)$$

$$Cd^{+2} + 2e = Cd \qquad (3)$$

$$Cd(S) + Se(S) \Longleftrightarrow CdSe \qquad (4)$$

3.2.2 Substrate Cleaning

Cleanliness of the substrates, for the thin film deposition is one of the most important factors for obtaining the reproducibility of the properties. It also affects the adherence, smoothness, brightness and uniformity of the film. The technique to be adopted for cleaning depends upon the nature of the substrate, degree of cleanliness required and nature of contaminants to be removed. The common contaminants are grease, adsorbed water, air-borne dust, lint and oil particles.

Cleaning is the process of breaking of adsorption bonds between the substrate and the contaminants without damaging the substrate. There are many methods to supply energy for breaking such bonds, such as heating, bombarding by ions, chemical action and scrubbing. Following procedure was adopted to clean the stainless steel substrates.

i. First substrates were polished with the emery paper.

ii. Then substrates were cleaned with soap solution and washed with flowing water.

iii. Substrates were rinsed in the double distilled water.

iv. Substrates were ultrasonically cleaned.

v. Finally drying of substrates was done in the vapour of isopropyl alcohol, with the help of special stand kept in a steel box, which was heated for few minutes.

In electrodeposition technique, it is very essential to have very clean substrates. Such type of substrates were preserved in a box free from moisture, dust etc.

3.2.3 Preparation of Solution

Appropriate weights of $CdSO_4$ and SeO_2 were taken on semimicrobalance so as to achieve the particular concentrated solution. Then they were dissolved in double distilled water. This solution was used after 10-12 hours for the deposition of thin films.

3.2.4 Time Period of Deposition Solution

When the deposition solution was used just after the preparation of solution, then it was observed that the thin films were not good. However, when the solution was used after 10-12 hours for deposition, then it was observed that the films were good even from the first film and also showed greater PEC effect. Why?

what is good? this is very qualitative word. The exact meaning should be brought about

3.2.5 Effect of Counter Electrode on Deposition

When the stainless steel was used as counter electrode instead of graphite then it was observed that the

uncalled for

? does This mean that adhesion of films to the substrate was harder. ?

films were very much sticky and uniform as compared to the films obtained by graphite as a counter electrode. These films also showed greater PEC effect.

3.2.6 Variation of Current Density With Time

Here the substrate of the size 9 X 14 cm^2 was used. The deposited film area was near about 100 cm^2. The

not matching ?

current varies between 15 and 60 mA. Variation ? with what ? of current density with deposition time of CdSe alloyed films is shown in Figure 3.4. From the figure, it is seen that the deposition current drastically decreases initially and then slowly decrease with deposition time.

3.2.7 Annealing Effect

The films deposited at potential -0.65 V (vs SCE) with deposition period of 60 minute were annealed at 370°C. After annealing, CdSe/stainless steel contact is ohmic. After annealing it was observed that the films were more stable in polysulphide solution. Annealed films also showed greater PEC effect.

3.2.8 Microstructure

Micrographs of CdSe films of two different deposition potentials are shown in Figure 3.5. The magnification of micrographs is 500X. The films deposited at -0.65 V (vs SCE) are uniform, dense and packed arrangement of grains

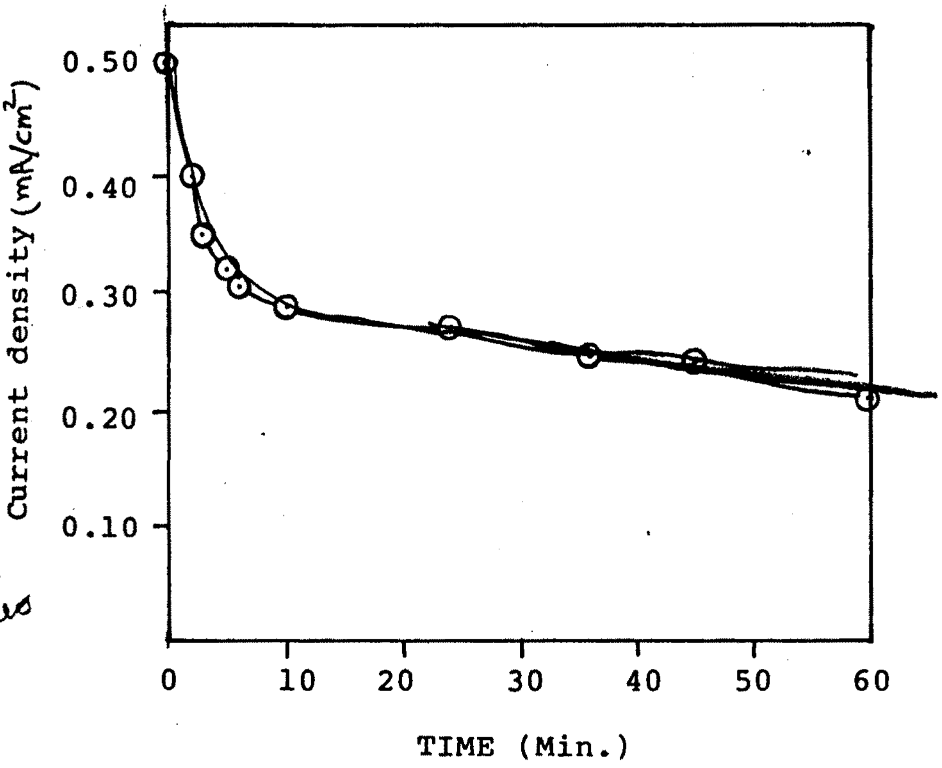

Smooth curves

Fig.3.4. Variation of current density with time during deposition of CdSe film

a) Film at -0.50 V (vs SCE)

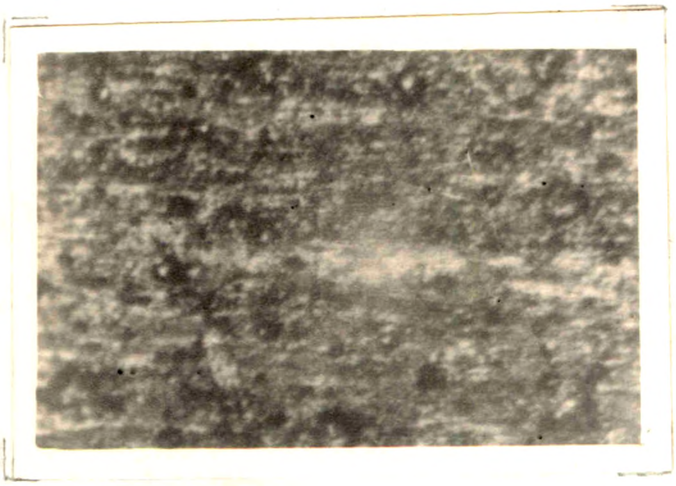

b) Film at -0.65 V (vs SCE)
before annealing

c) Film at -0.65 V (vs SCE)
after annealing

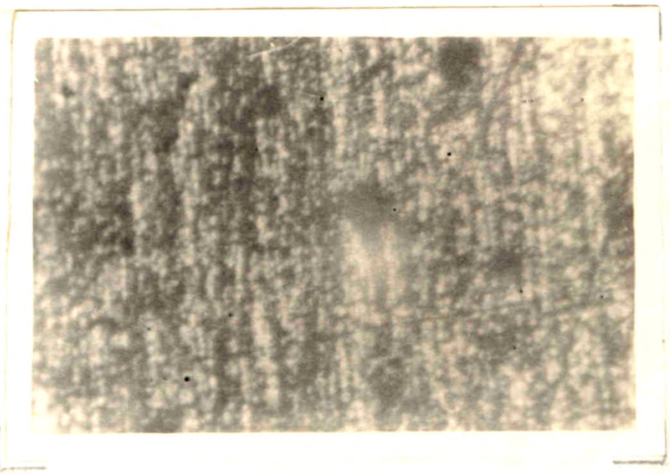

Fig.3.5. Microphotographs of electrodeposited CdSe films.

than films deposited at -0.50 V (vs SCE). Micrograph of the annealed film deposited at -0.65 V (vs SCE) shows closed packed arrangement (Figure 3.5c).

3.2.9 X-Ray Diffraction (XRD)

The study was carried out for the film prepared on to stainless steel substrate. The XRD pattern of CdSe film was recorded by using X-ray diffraction model Phillips PW-1710. The XRD diffraction pattern for the CdSe film deposited at -0.65 V vs SCE is shown in 3.6. The presence of sharp peaks shows that the film is polycrystalline in nature. Comparison of observed 'd' values with standard 'd' values from ASTM data [33] are listed in Table I. The observed 'd' values are well matched with standard 'd' vlaues of hexagonal structure of CdSe. Hence the structure of material is hexagonal. The lattice parameters a = 4.297 A and c = 7.2819 A were calculated using the formula for hexagonal.

$$\frac{1}{d^2} = \frac{4}{3}\left[\frac{h^2 + hk + k^2}{a^2}\right] + \frac{l^2}{c^2}$$

where - h, k, l are the Miller indices.

How the XRD work was done is not clear

a) Was CdSe a single crystal

b) If not what was the grain size?

c) How did you eliminate SS peaks?

TABLE - I

XRD Data of Electrodeposited CdSe Film With Lattice Parameters (Structure Hexagonal)

a_o = 4.297 A

c_o = 7.2819 A

d values observed	d values from ASTM data	hkl	I/I_{max}
3.261	3.149	220	10.08
2.025	1.980	103	42.35
1.792	1.800	201	42.35
1.214	1.221	301	13.91

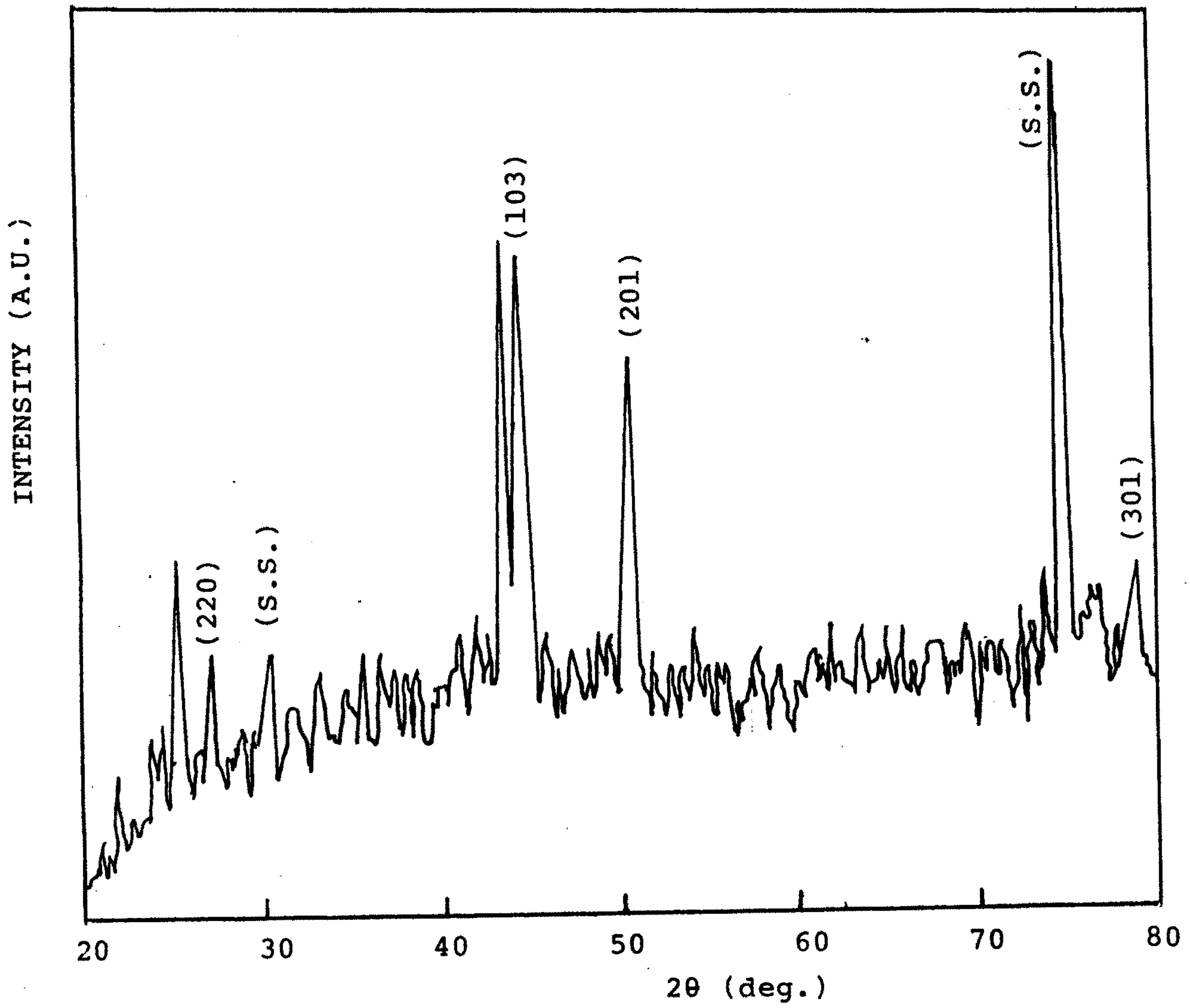

Fig.3.6. XRD pattern of CdSe film electrodeposited at −0.65 V (vs SCE).

3.2.10 Construction of SC-SEP Solar Cell

The cell consisted of two compartments made up of plastic boxes with 10 cm X 8 cm area cut on their sides. The CdSe septum electrode was then fixed between two compartments, by using adhesive cream Araldite. The glass was fitted on front side of the first compartment to illuminate the film. The compartment adjacent to the tungsten halogen lamp (500 W) was filled with 1 M 500 ml polysulphide (Na_2S-NaOH-S) solution in contact with n-CdSe film. The other compartment (dark) was filled with a redox couple like $FeCl_3$ (500 ml). The concentration of $FlCl_3$ was varied. The counter electrodes in both compartments were graphite plates. To increase the area of counter electrode in compartment I without blocking the incident light on the film, following arrangement was done : Two graphite plates were fitted at the two sides and one plate at the centre and these three plates were joined by putting a plate at bottom of the box. These plates were interconnected by silver pest for electrical contact and by adhesive cream Araldite. So maximum part of film was illuminated. The area of graphite electrode in both the compartments was near about 120 cm^2. The semiconductor septum solar cell diagram is shown in Fig.3.7. The idea for construction of large size redox storage cell was taken from the work of Pawar et al. [34].

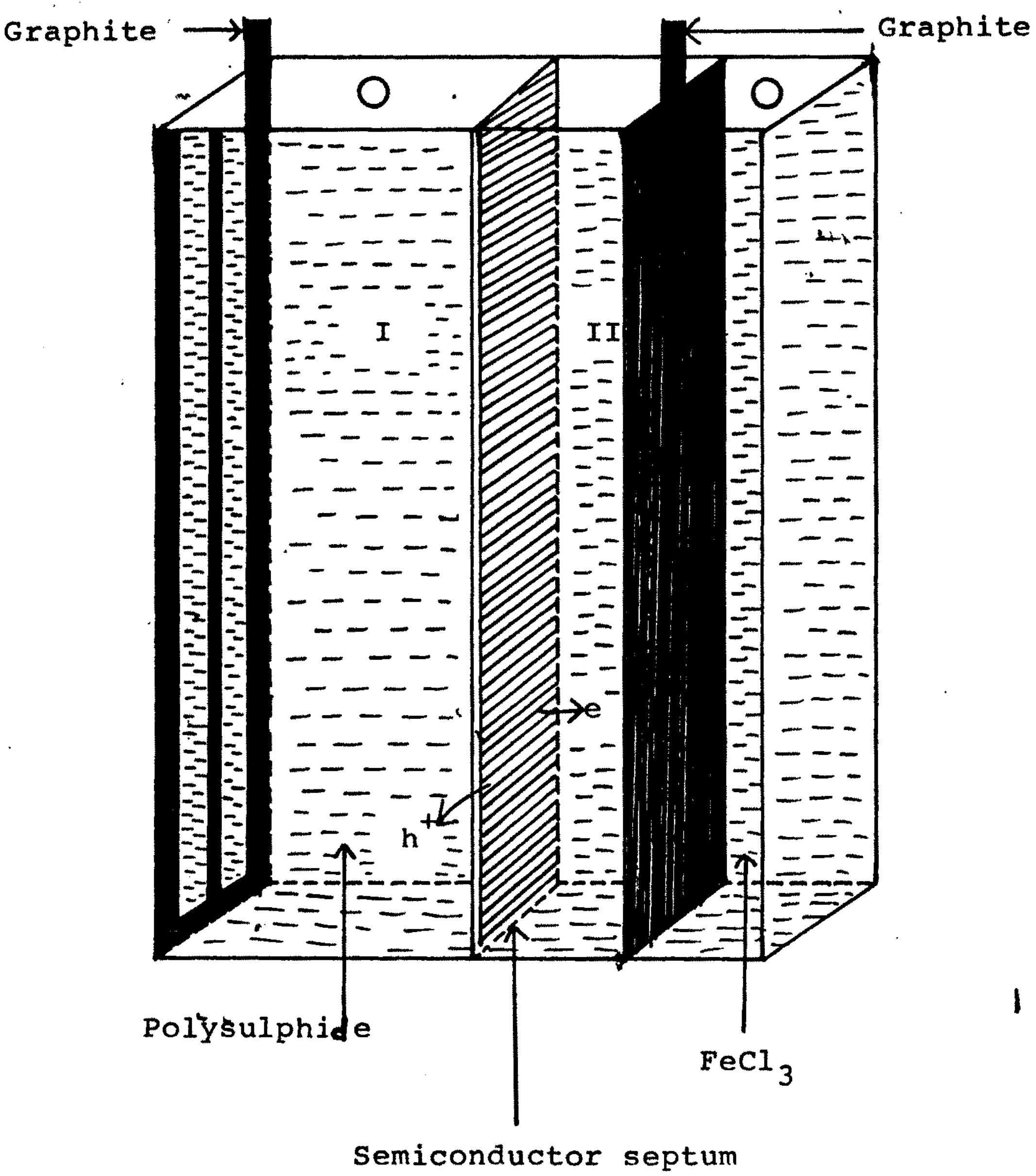

Fig.3.7. SC-SEP solar cell.

3.2.11 Storage in the form of Electrical Energy (working of SC-SEP cell)

Fig.3.8(a) and 3.8(b) show the SC-SEP solar cells under charging and discharging mode respectively. Open circuit voltage and short circuit currents of the cells were measured between two graphite electrodes with digital multimeter. The configuration of the cell was as follows :

Grphite/(Na_2S-NaOH-S)/Semiconductor(CdSe)//Metal/$Fecl_3$/Graphite
I Compartment II Compartment

The light source was 500 W tungsten filament lamp. Water filter was interposed between the lamp and the cell to avoid excessive heating. Intensity of light was measured with Suryamapi.

The semiconductor septum cell under illumination causes generation of electron-hole pairs, the electrons jump into the conduction band form valence band. The electron further moves towards the bulk of the semiconductor and via metallic substrate travels into the other compartment where it is received by the oxidized species and gets reduced. The oxidized species get either reduced to lower oxidation state or to metal. These species can again be reoxidized by transfering an electron to the metal electrode in compartment II, in dark, while hole moves towards the surface of the semiconductor and accepted by the reduced

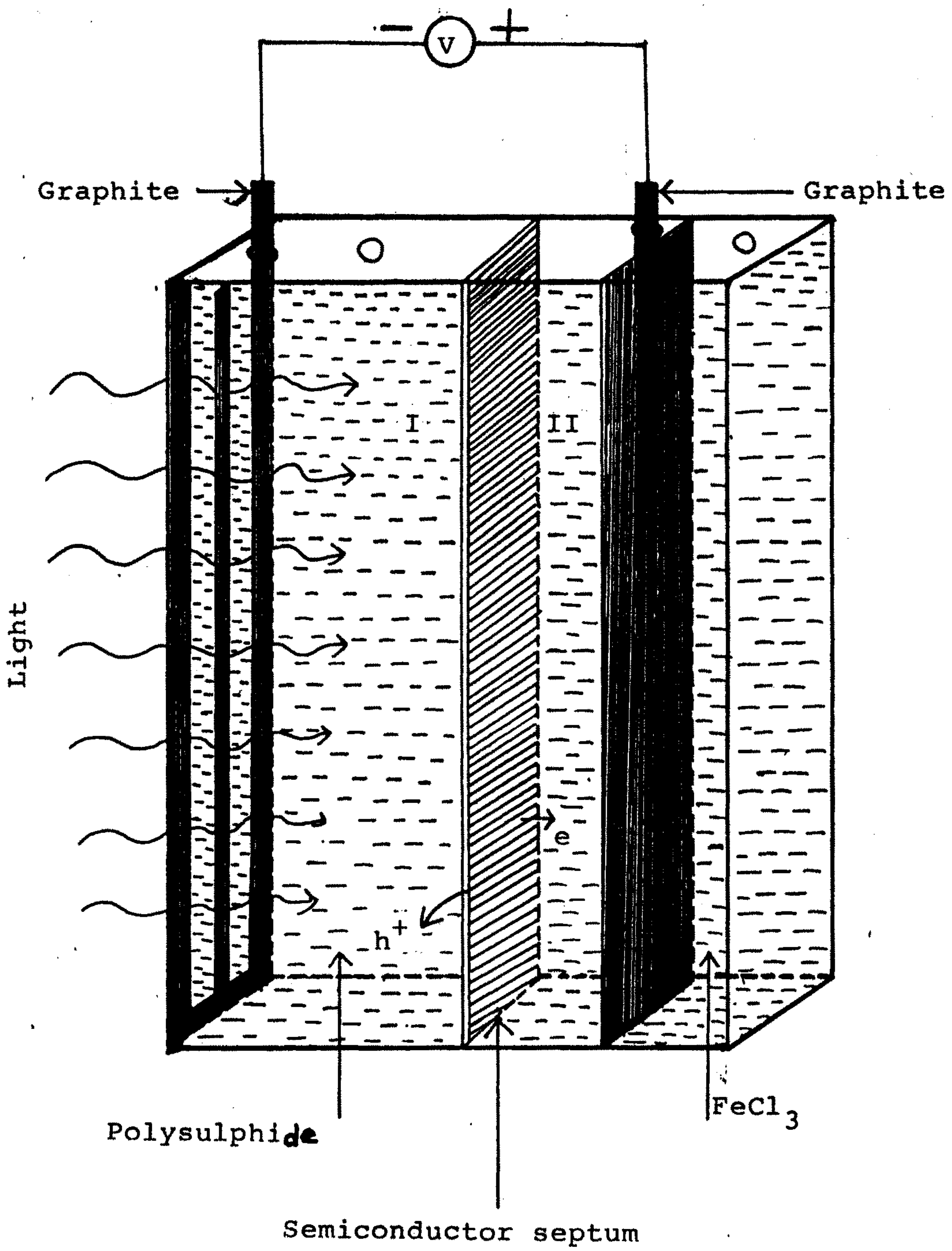

Fig.3.8.(a) SC-SEP solar cell under charging mode.

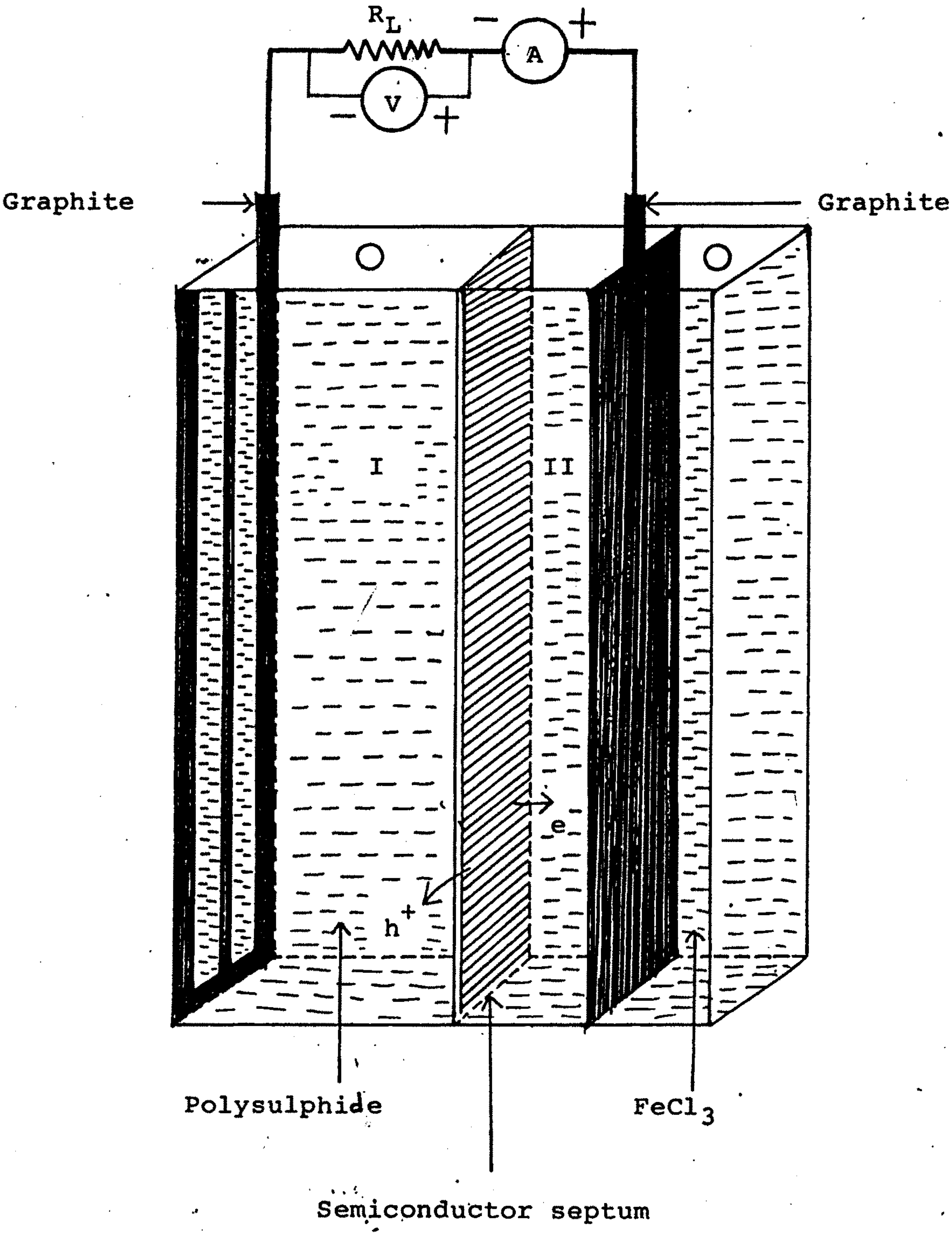

Fig.3.8.(b) SC-SEP solar cell under discharging.

species present in compartment I and get oxidized. In dark (discharging mode), these oxidized species accept electrons from compartment II, resulted in the electricity flow through external load.

When the semiconductor septum solar cell is illuminated, the overall reactions may be written as

$$\text{Semiconductor} \rightleftharpoons e^- \text{ (C.B.)} + h^+ \text{ (V.B.)}$$

C.B and V.B represent conduction band and valence band of semiconductor respectively.

In compartment I (light)

$$2h^+ + S^{2-} \longrightarrow S$$

$$S + S^{2-} \longrightarrow S_2^{2-}$$

$$2h^+ + 2S^{2-} \longrightarrow S_2^{2-} \quad \text{net reaction}$$

In compartment II (dark)

$$Fe^{3+} + e^- \longrightarrow Fe^{2+}$$

In general

$$n.L^{-1} + n.h^+ \rightleftharpoons L^{-(n-1)} \quad \text{....compartment I}$$

$$n.M^n + n.e^- \rightleftharpoons n.M^{n-1} \quad \text{....compartment II}$$

Where L and M denotes various redox species present in compartment I and compartment II respectively. During charging these reactions shift from left to right and in the opposite direction during discharging. Thus, the system could be charged photoelectrochemically and discharged elecrtrochemically for the production of electricity upon demand as shown in Fig.3.9.

If contacting electrodes and electrolytes are the same in both compartments, no net chemical change takes place, because the reactions are opposite but equal. Such a cell functions mereley as a transducer, changing light into electrical energy.

3.2.12 Criteria for Selection of Redox Couples

A redox flow cell (or battery) in one in which the chemical species participate in storing electrical energy and regenerate the energy when needed. The cell is charged with the input of electrical energy to drive the overall cell reaction. The oxidized species are produced in one half-cell (anodic compartment) and the reduced species are produced in another half-cell (cathodic compartment).

The most serious limitation for redox cell batteries is in the selection of practical redox couples to produce a complete redox cell. This is because a number of demanding conditions have to be fulfilled by candidate redox couple in order to be useful for the formation of a complete redox cell.

1. The thermodynamic potentials of the two redox couples have to be sufficiently different to give an acceptable

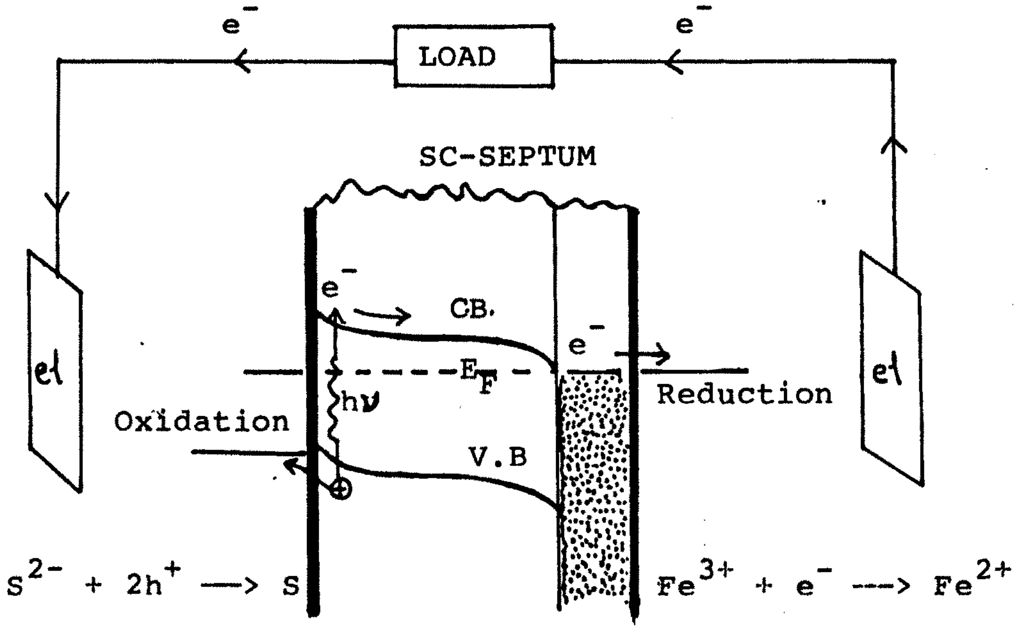

Fig.3.9. The mechanism and operation of the SC-SEP cell.

open circuit cell potential; in practice more than one volt difference is required. Lower open circuit potential differences necessiate an excessively high number of cells, which result in high capital costs, increased membrane crossover probability and lower "round trip" efficiency.

2. The kinetics of the redox couples must be fast, in addition, when the potential of any of the redox couples lies outside the range of thermodynamic stability of water, the kinetics of water decomposition (H_2/or O_2 evolution) have to be slow at the operating conditions, not only at the inert electrode but also within the electrolyte bulk.
3. All the species in the redox couple must be soluble under all operating conditions (typically the solubility should be higher than 1 mole (litre).
4. The reactants should be readily available and inexpensive.
5. The reactants should be environmentally acceptable under normal operating conditions and under any anticipated system disfunctions.
6. It is important that the two redox couples be compatible with each other in regard to their separation requirements and the mechanism by which ionic conductivity takes place at the membrane.

3.3 PROPERTIES OF SC-SEP SOLAR CELLS:RESULTS AND DISCUSSION

3.3.1 Variation of I_{sc} and V_{oc} with Light Intensity

The photoresponse is measured in terms of the PEC cell parameters, namely open circuit voltage (V_{oc}) and short circuit current (I_{sc}). The variation of I_{sc} with white light intensity is shown in Fig.3.10. Here only compartment I was filled with polysulphide solution and area of the film was 80 cm². The plot is found to be linear and is in good agreement with the theory. The linear nature of the plot leads to express them in a mathematical relation.

what about saturation for intensities range of 30 to 65 mW/cm²

with a 500 W lamp how did you measured energy -

$$I_{SC} + CI_L$$

where I_L is the intensity of light and C is proportionality constant and it dependent on the fraction of light utilized for the generation of charge carriers and effective separation of the generated charge carriers. The slope of the plot give the magnitude of C.

Open circuit voltage (V_{OC}) of the PEC cell was also found to vary with the light intensity. Figure 3.11 shows the variation of V_{OC} with white light intensity. // ?

3.3.2 Dark and Photo Voltage and Current for Number of Cells

When only compartment I of the number of cells were filled with polysulphide and illuminated with light of

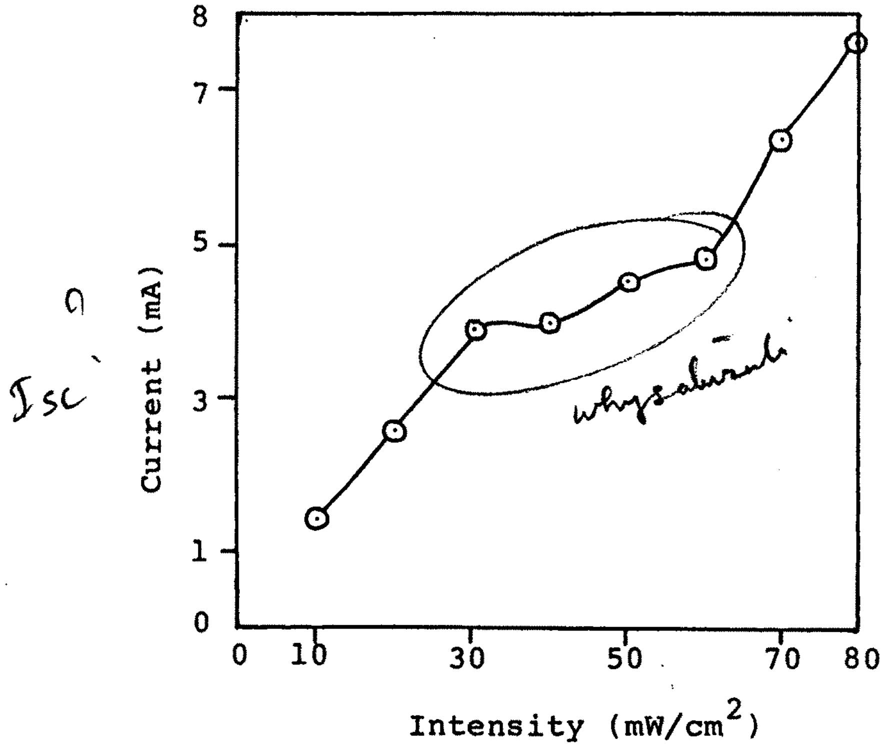

Fig.3.10. Variation of current with intensity

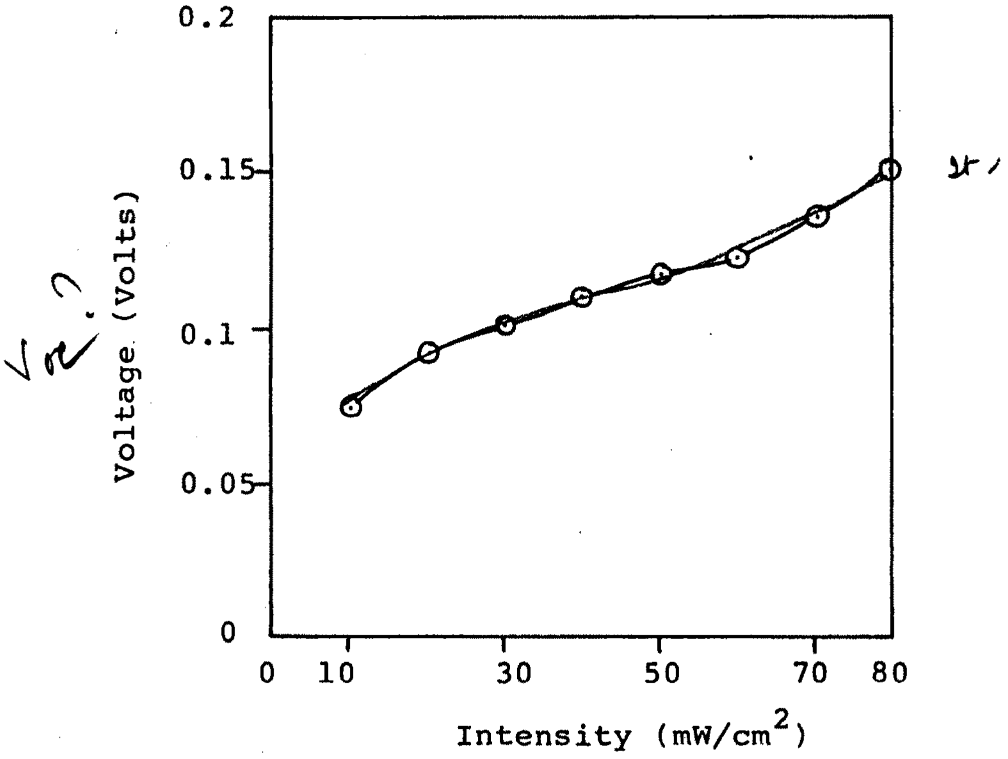

Fig.3.11. Variation of voltage with intensity.

intensity 80 mW/cm^2, then on an average the variation in voltage and current are as given in Table II and Table III.

Table shows the results for the films of area 100 cm^2 and that of Table III for area 80 cm^2.

Table II Dark and Photo Voltage and Current for 100 cm^2 area of the film

Dark Voltage V (volts)	Dark Current I (mA)	Photovoltage V_{ph} (volts)	Photocurrent I_{ph} (mA)
0.037 ± 0.006	0.02 ± 0.001	0.232 ± 0.032	13.15 ± 2.75

Table III Dark and Photo Voltage and Current for 80 cm^2 area of the film

Dark Voltage V (volts)	Dark Current I (mA)	Photovoltage V_{ph} (volts)	Photocurrent I_{ph} (mA)
0.012 ± 0.001	0.05 ± 0.001	0.136 ± 0.042	7.3 ± 1.5

From Table II and III, it is seen that for larger area of the film, the photovoltage and photocurrents are large. Thus current depends upon the area of the semiconductor film.

3.3.3 Effect of Counter Electrode in PEC Cell

The photo currents for two different counter electrodes were as shown in Table IV

Table IV Photo Currents for two different counter electrodes at constant intensity

Counter Electrode	Photo Current I_{ph} (mA)
Graphite	6.5
St. Steel	0.52

For table IV it is observed that the photocurrent for stainless steel counter electrode is very small as compaired to graphite counter electrode. This is due to the fact that Fermi levels of counter electrode and substrate are same. So graphite or other metal, different than St-steel can be used in PEC cells as counter electrode. Photo-current also depends upon the area of the counter electrode.

3.3.4 Cell Formed With 1 M $FeCl_3$ Electrolyte

(A) Area of the Semiconductor Septum Film = 100 cm^2

The open circuit voltage and short circuit currents were measured between two graphite electrodes before and after one hour charging the semiconductor septum cell. The average values of cell voltages and currents for number of cells are listed in Table V. The intensity of light was 80 mW/cm^2.

Table V Cell Formed With 1 M $FeCl_3$ and area of Semiconductor Septum Film = 100 cm^2

Voltage of cell before charging V_{OC}(volts)	Voltage of cell after 1 hr. charging V_{OC} (volts)	Short Circuit current before charging I_{sc} (mA)	Short Circuit current after 1 hr. charging I_{sc} (mA)
0.545±0.110	0.967±0.087	10.87±2.7	288±50

When current was measured after charging the semiconductor septum solar cell, it was observed that the current drastically decreased initially and then slowly. The values of the currents given in table V are the initial values during the measurement of currents. For different cells the values of voltage and currents are nearly same.

The magnitudes of voltage and currents of semiconductor septum storage cell depend on the following factors [35].

(i) Adaptability of electrode/electrolyte.
(ii) Difference in redox Fermi levels.
(iii) Area of Semiconductor septum.
(iv) Total number of charges stored in compartments.

(i) Adaptability of electrode/electrolyte

The nature of electrode/electrolyte interface is dependent on particles present on the surface of the electrode and the forces between the particles and the ions in an electrolyte. These forces are different at the interphase region compared with forces in the bulk. As per nature of the forces, the solid-electrolyte interface cab be classified into three types [36].

(i) electronically and chemically inert interface
(ii) chemically inert but electronically active interface,
and
(iii) corrosive interface.

In case of first type of interface, for example, glass rod immersed into an electrolyte solution, there will not be either charge transfer reactions or the chemical reactions. A stable metal into an electrolyte gives the second type of interface in which charge transfer reaction occurs across the interface but the interface is chemically inert. The last type of interface, called as corrosive interface, involves both the charge transfer reactions as well as chemical reactions across the interface. Consequently a metal electrode does not remain as a metal electrode. We are interested in the second type of interface. The properties of interface depend on arrangement of particles and the forces operating on them. Since new forces exist near the phase boundary, new structure would tend to exist. Theoretical treatment of metal-electrolyte interface has been extensively reviewed [37-43].

A charged surface in contact with an electrolyte solution is expected to attract ions of opposite charge and to repel ions of like charge, establishing an ion atmosphere in the immediate vicinity of the surface. Two parallel layers of charges are formed, the charge on the surface itself and the layer of oppositely charged ions near the surface. This structure is called the electric double layer.

The direction of charge transfer depends on the metal, but in general charge separation occurs and an electric potential difference is developed between the metal and electrolyte. Hence, we get different cell voltages and currents from different electrodes in an electrolyte. Here the graphite electrode was used.

(ii) Difference in Redox Fermi Levels

The cell voltage depends on electrolytes present in compartments. We know that there are different electrolytes in compartment I and compartment II. The polysulphide electrolyte is present in compartment I (photoanode side) and $FeCl_3$ electrolyte is present in compartment II (dark compartment). These electrolytes in compartments I and II of cell are such that their chemical potential levels

$E_{F,redox1}$ and $E_{F,redox2}$ do not coincide. This is necessary, first, to raise the output voltage and second, to use more effectively the energy of light generated carriers (or it is some times said to completely use the semiconductor forbidden band width).

Upon illumination, the storage cell get charged owing to the occurrence of reactions.

$Red_1 + h^+ \longrightarrow OX$ .... (comp. I)

$OX_2 + e^- \longrightarrow Red_2$ .... (comp. II)

Therefore, the $E_{F\ redox1}$ and $E_{F\ redox2}$ levels shift still further from each other. Thus, the cell is charged and cell voltage depends on the position of the band edges of semiconductor and Fermi levels of redox system.

(iii) Area of Semiconductor Septum

The semiconductor septum electrode acts as phtoanode as well as separator of two aqueous compartments. The short circuit current of cell depends on area of separator. It we use large area then charging and discharging rate will be large. In case of starting battery, for heavy discharge within few seconds, area of septum cell should be large. From table VII it is seen that for 100 cm^2 area of semiconductor septum film current is 300 mA and that for 80 cm^2 area it is 200 mA.

(iv) Total number of charges stored in compartments

The short circuit current of cell depends on number of charges stored in compartments. The maximum amount of electricity delivered by a cell is referred to as ampere-hour (Ah) capacity. The Ah capacity depends on volume of electrolytes and valencies of metal ions. From table VIII, it is seen that the capacity of cell is more for higher concentration of electrolytes.

The charging curves for 5 number of cells were recorded and the mean curve is shown in Fig.3.12, with error flag. The nature of the graphs shows that the charging is exponential. The nature of the curves for all the cells are more or less same.

(B) Area of the Semiconductor Septum Film = 80 cm^2

The open circuit voltage and short circuit currents for number of cells in an average are listed in table VI. The intensity of light was 80 mW/cm^2.

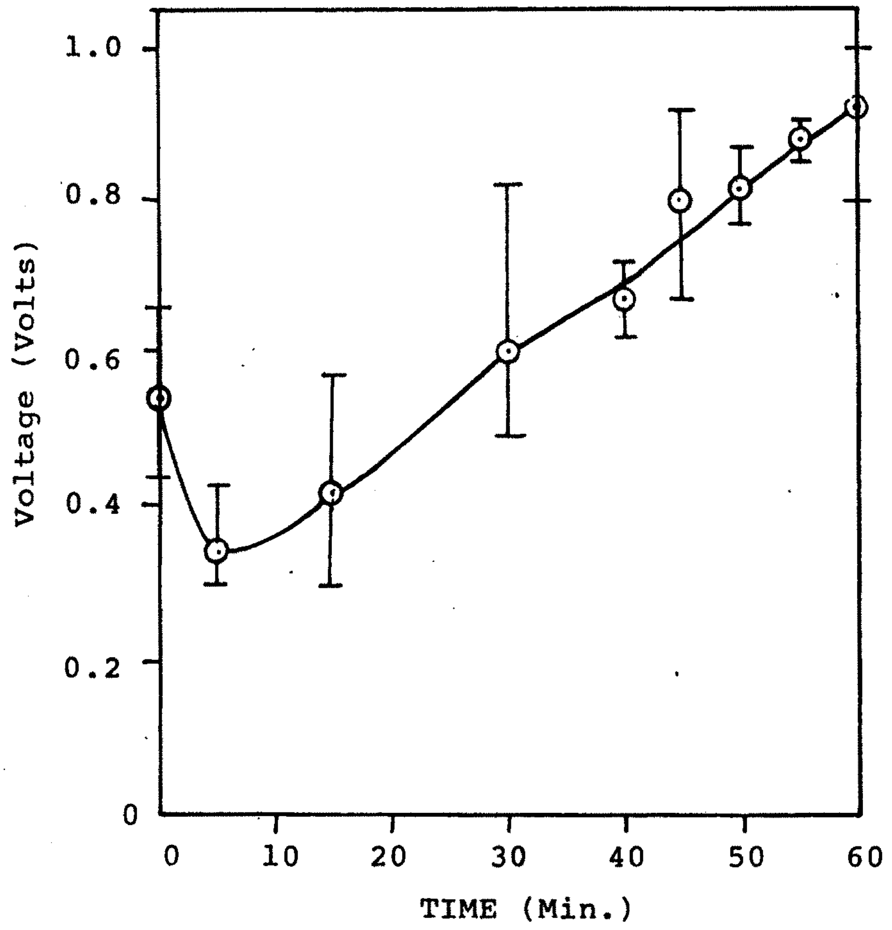

Fig.3.12. Charging curves for 5 no. of cells formed with 1M $FeCl_3$ and area of semiconductor 100 cm^2.

Table VI Cell Formed with 1 M $FeCl_3$ and Area of Film = $80cm^2$

Voltage of cell before charging V (volts)	Voltage of cell after 1 hr. charging V (volts)	Short Circuit current before charging I_{sc} (mA)	Short Circuit current after 1 hr. charging I_{sc} (mA)
0.443±0.021	0.785±0.100	19.0±2.2	186 ± 10.00

The charging curves for 3 numbers of cells were recorded and the mean curve is shown in Fig.3.13, with error flag. In the charging mode it was observed that initially there is a decrease in open circuit voltage till the equilibrium is established. Then it increases rapidly with time and attains saturation value.

Table VII shows the values of open circuit voltage and short circuit current of the semiconductor septum solar cell for the areas of semiconductor film 100 cm^2 and 80 cm^2 with 1 M $FeCl_3$ concentration.

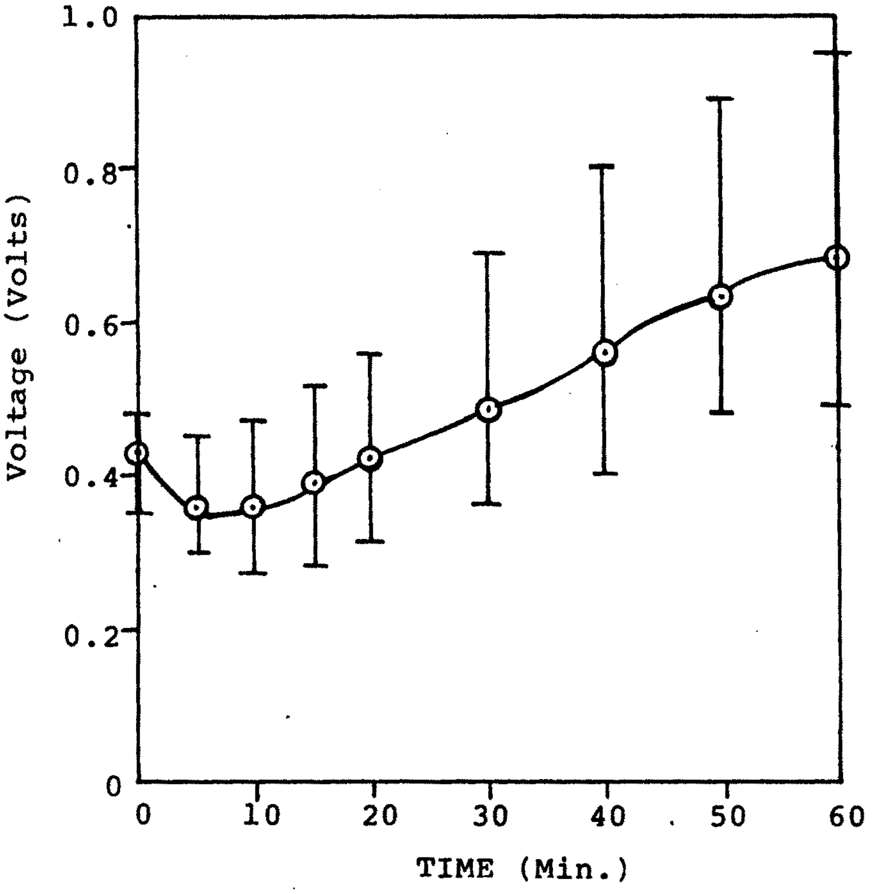

Fig.3.13. Charging curves for 3 no. of cells formed with 1 M $FeCL_3$ and area of film 80 cm^2.

Table VII System Formed with 1 M Polysulphide (comp. I) and 1 M $FeCl_3$ (comp. II)

Area of Semiconductor Septum Film	Current after 1 hr. charging I_{sc} (mA)	Voltage after 1 hr. charging V_{oc} (volts)
100 cm^2	$\simeq$ 300	0.9
80 cm^2.	$\simeq$ 200	0.9

3.3.5 Cell Formed with 0.5 M $FeCl_3$ Electrolyte

In this cell 0.5 M concentration of $FeCl_3$ in compartment II and 1 M polysulphide in compartment I was used. Area of semiconductor septum film was 80 cm^2. Intensity of light was 80 mW/cm^2. The cell voltage 0.620 volts and short circuit current 83 mA after one hour charging were observed. Fig.3.14 shows charging curve.

3.3.6 Cell Formed with 0.1 M $FeCl_3$ Electrolyte

The cell voltage 0.602 volts and short circuit current 22 mA after one hour charging were observed. Fig.3.15 shows charging of cell.

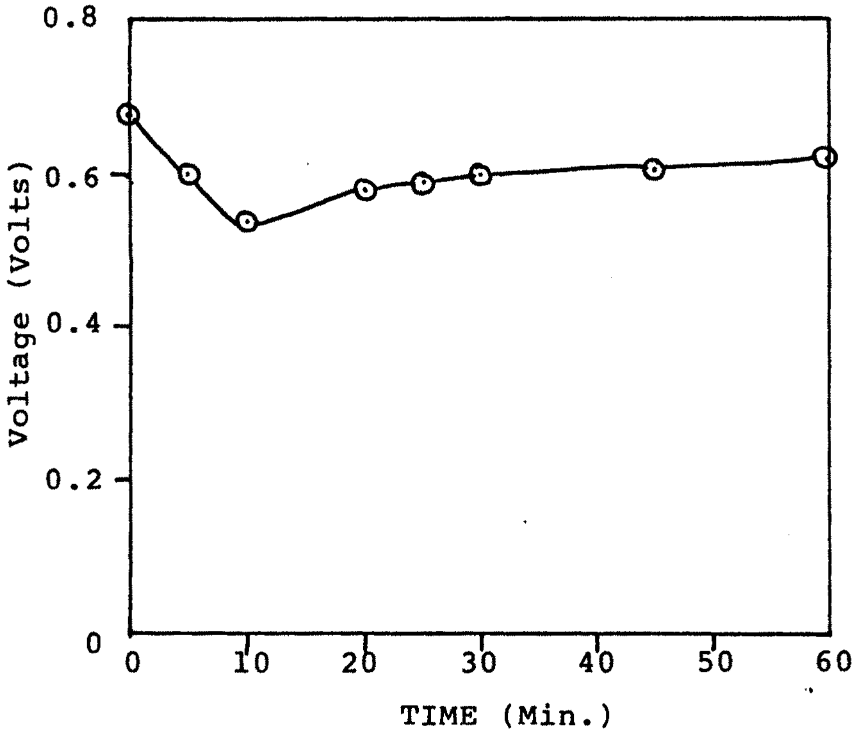

Fig.3.14. Charging curve for 0.5 M $FeCl_3$ cell area of semiconductor film 80 cm^2.

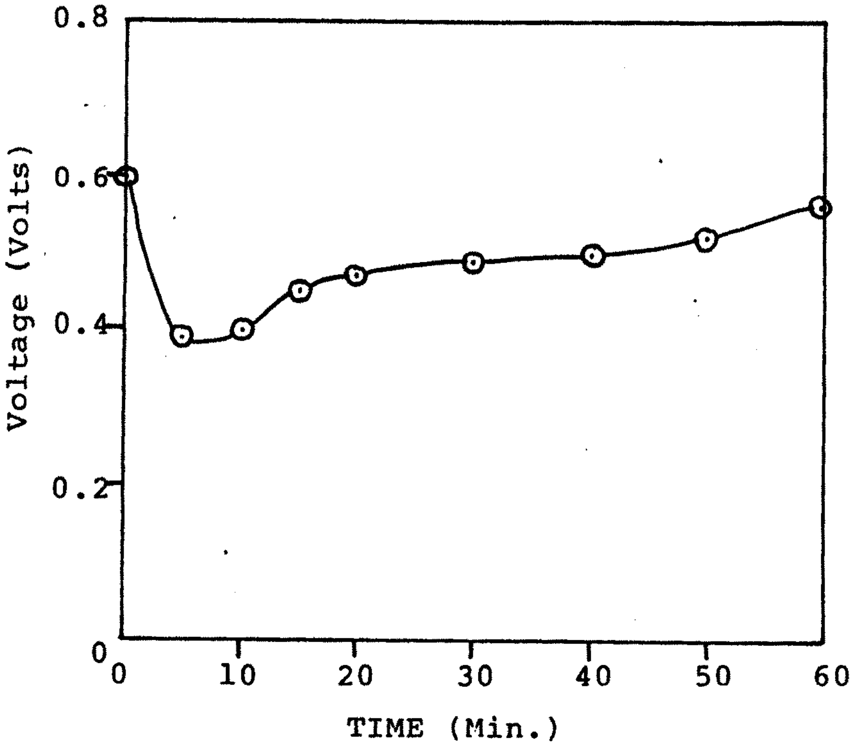

Fig.3.15. Charging curve for 0.1 M $FeCl_3$ cell area of semiconductor film=80 cm^2

Table VIII Area of Semiconductor Septum Film = 80 cm^2

Concentration of $FeCl_3$	Current after 1 hr. charging I_{sc} (mA)	Voltage after 1 hr. charging V_{oc} (volts)
1.0 M	200	0.9
0.5 M	80	0.7
0.1 M	22	0.6

3.3.7 Discharge Across Load Resistance

After charging the semiconductor septum solar cell for one hour, the cell was allowed to discharge through 1 KΩ resistance.

Under the illumination the oxidation reaction takes place in compartment I while reduction takes place in compartment II.

During the discharging of the cell the reduced species in compartment II can again reoxidized by transferring an electron to the metal electrode and oxidised species in compartment I accept electrons from the compartment II through the external circuit, which results in the electricity flow through external load.

The discharging magnitudes of current and voltage were noted for different concentration of $FeCl_3$ in the compartment II. 1 M polysulphide was kept constant in compartment I. The value of load resistance was $R_L = 1$ K .

For 1 M $FeCl_3$, the discharging curve is shown in Fig.3.16.

For 0.5 M $FeCl_3$, the discharging curve is shown in Fig.3.17.

For 0.1 M $FeCl_3$, the discharging curve is shown in Fig.3.18.

There was a continuous and nearly constant power generation through the external load for 4 hours as shown in Fig.3.19.

3.3.8 Corrosion of Semiconductor Septum Cell Formed with $FeCl_3$ Electrolyte

For a practical long-life semiconductor septum solar cell, the semiconductor electrode must be stable against : (i) dissolution, (ii) photocorrosion and (iii) electrochemical corrosion.

Semiconductor septum also must be stable against corrosion due to electrolyte used in compartment II for a practical long life semiconductor septum solar cell.

The strong oxidising and reducing species in the

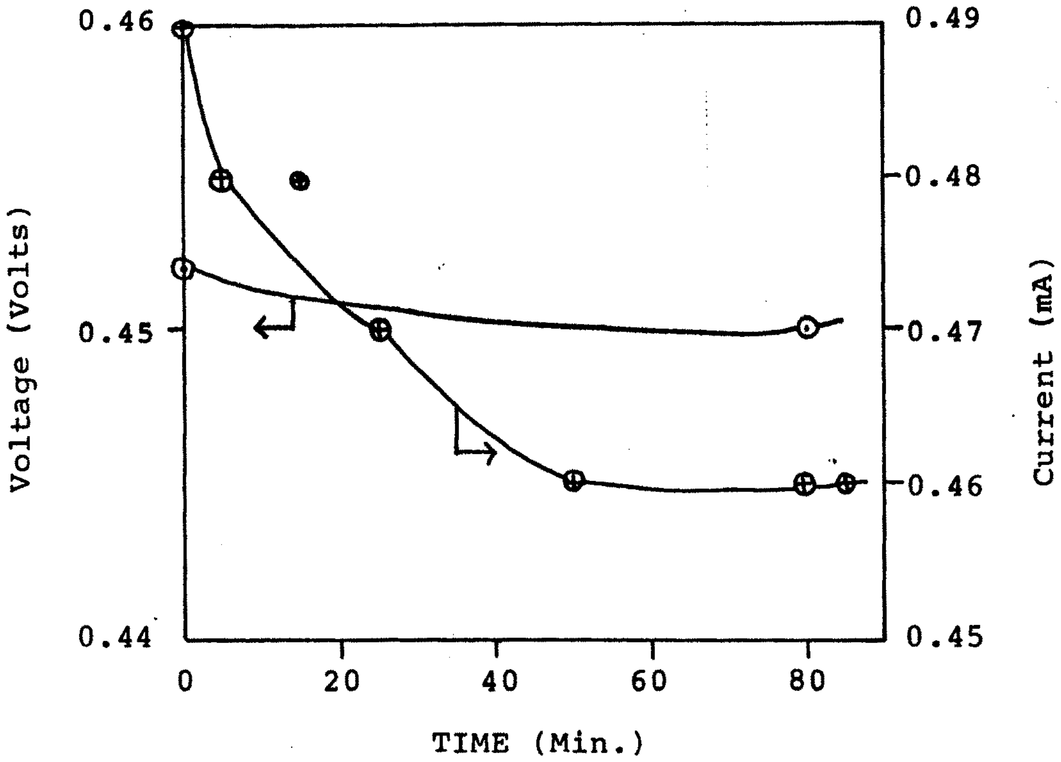

Fig.3.16. During discharging variation of current voltage with time across R_L=1K for 1 M $FeCl_3$.

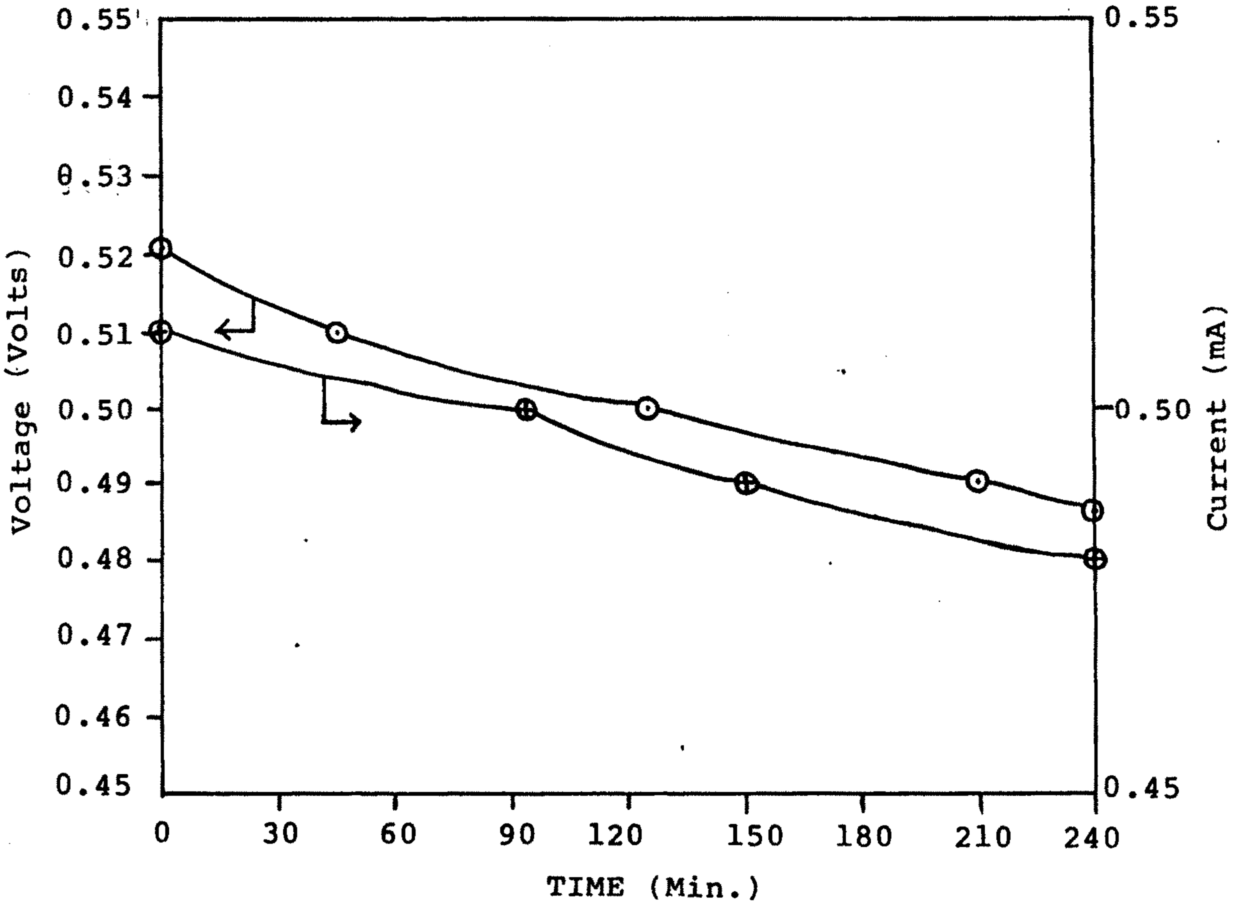

Fig.3.17. During discharging variation of current voltage with time across R_L=1K for 0.5 M $FeCl_3$.

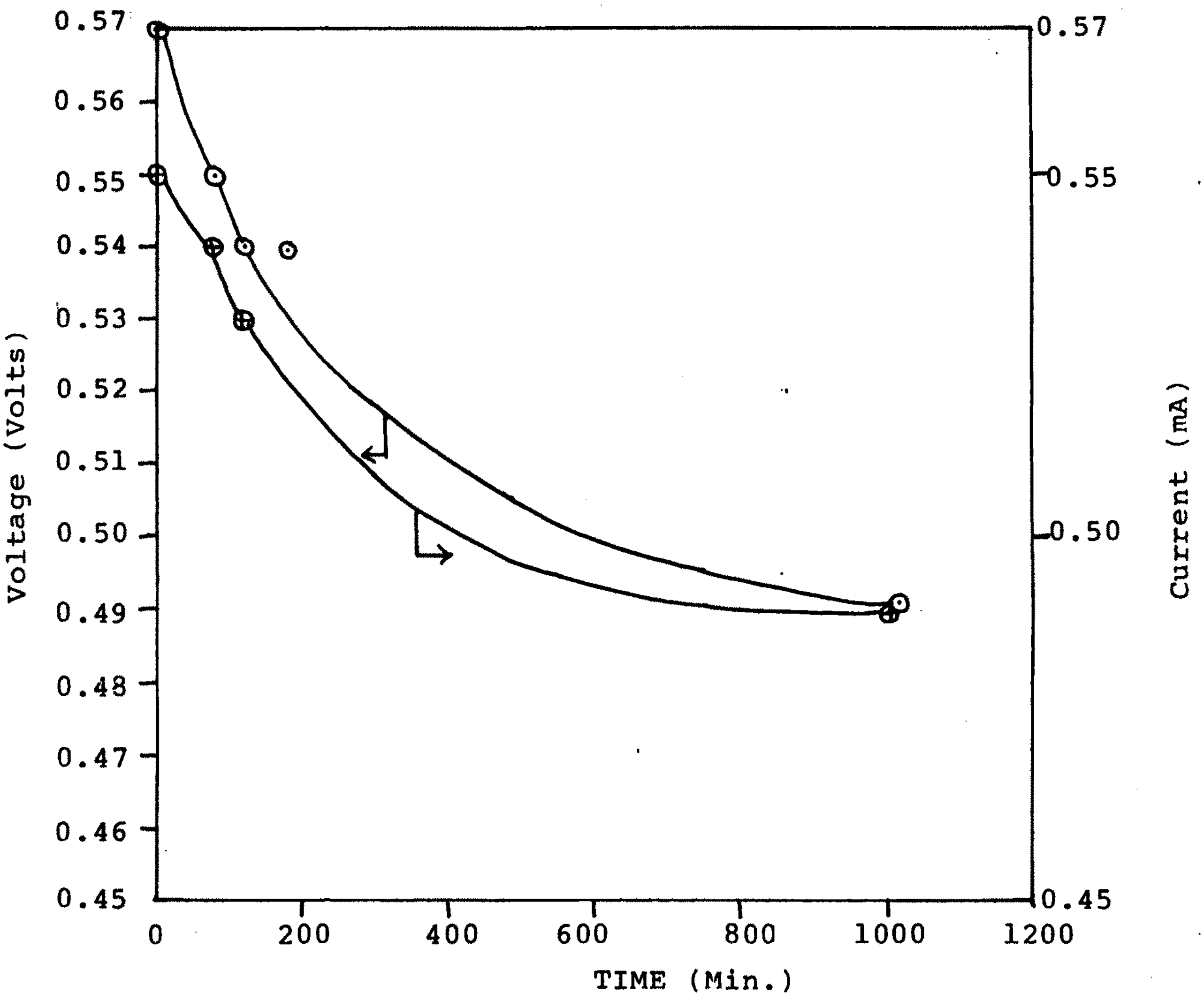

Fig.3.18. During discharging variation of current voltage with time across R_L=1K for 0.1 M $FeCl_3$.

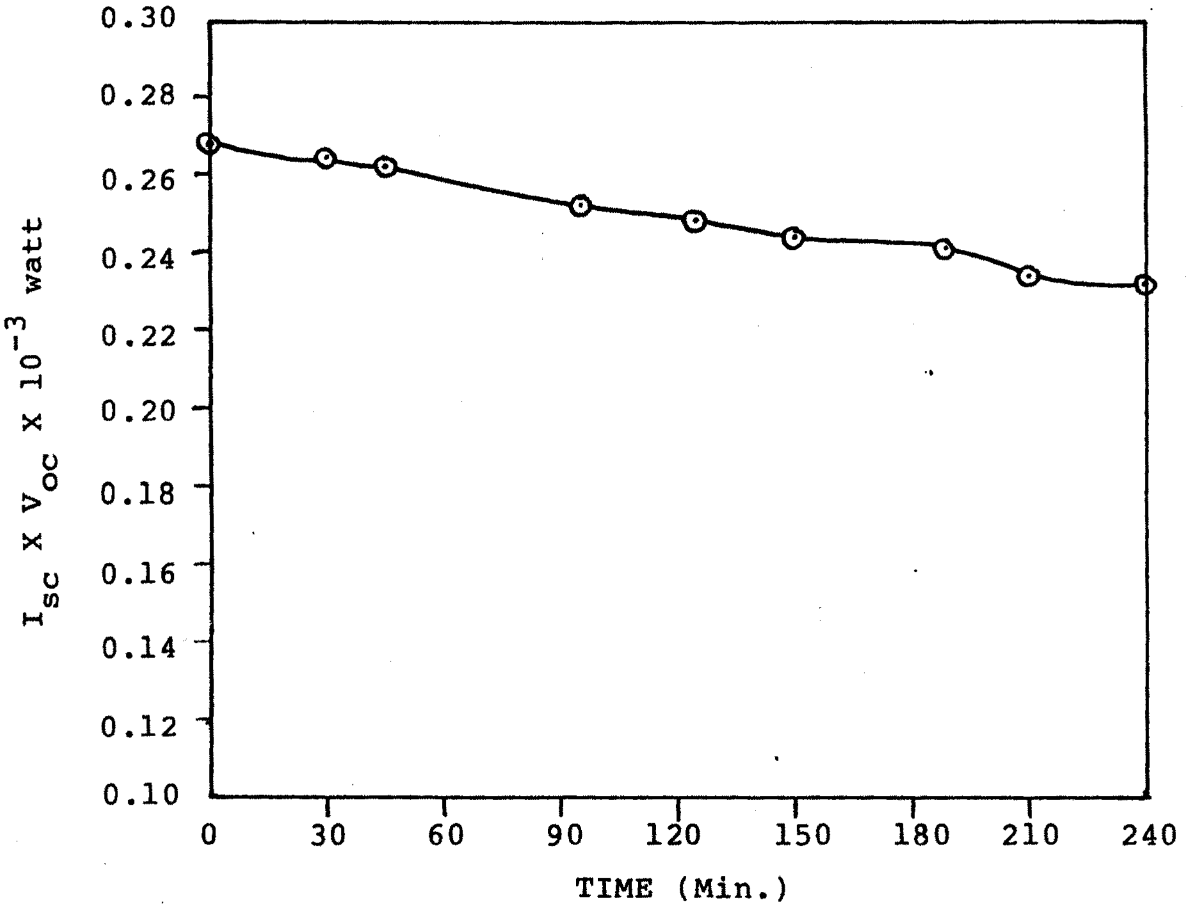

Fig.3.19. Output power with time for 0.5 M $FeCl_3$ in compartment II at 1K load.

electrode may corrode electrochemically which may be enhanced on illumination. Photogenerated or intrinsic electrons and holes in the semiconductor may accumulate at the electrode instead of getting injected into the electrolyte. This would either oxidise or reduce the semiconductor electrode ultimately leading to its dissolution. Brattain and Garrett [44, 45] were the first to study the corrosion of germanium. Subsequently many studies have been carried out [46, 47].

Almost all semiconductors corrode in varying degree both in dark and under illumination. The charge transfer reaction at the electrode-electrolyte interface is solely responsible for the dissolution or corrosion since it is a matter of common knowledge that semiconductors kept in vacuum do not corrode. In a broad sense, corrosion is the oxidation of a material without the passage of an electric current [46]. As a result, the oxidation of the solid electrode is accompanied by the reduction of some other component of the system. Most often the corrosion has an electrochemical nature. At the solid-liquid interface both cathodic and anodic reactions take place at the same rate :

$$M \longrightarrow M^+ + e^-$$

$$X + e^- \longrightarrow X^-$$

For metals, the above two reactions are regarded as completely independent. For semiconductor, the mobile charges of both Sings (e.g. electrons and holes) participate in the solid electrode - electrolyte exchange. So, the recombination and generation of free carriers must be taken into account. In a simplified model Gerischer [48] considered electrons or holes in s semiconductor as 'defects' which result in weakening of the covalent bonding between the constituent atoms of a semiconductor. Semiconductor decomposition can take palcein the following tow ways :

(a) Cathodic decomposition - Electrons participate in this reaction.

(b) Anodic decomposition - Holes participate in this reaction.

Thus one of the challenging problems in PEC cell is the stability of photoelectrode (thin film) in polysulphide. This problem was partially solved by several workers [49, 50]. Another challenging problem is the stability of semiconductor septum with $FeCl_3$ electrolyte. In semiconductor septum solar cell, as the concentration of redox couples increases, the number of ions increases and results in more current and strength of the battery. However, as concentration increases, there starts the corrosion of semiconductor septum solar cell. The mechanism of corrosion is studied and reported here.

3.3.8.1 Durability of Semiconductor Septum with Concentration of $FeCl_3$ Electrolyte

The Schematic diagram of the redox storage cell is presented in Fig.3.7. The configuration of the cell was as follows :

Graphite/(Na_2S-NaOH-S)/Semiconductor(CdSe)//Metal/$FeCl_3$/Graphite
I Compartment II Compartment

Under the illumination the mode of charging was studied. One of the cells after charging for one hour showed that the open circuit voltage (V_{OC}) = 1.01 volts and short circuit current (I_{SC}) = 200 mA. After 20 days it was observed that V_{OC} = 0.875 volts and I_{SC} = 130 mA. Concentration of $FeCl_3$ was 1 M in compartment II. After one and half month this cell was damaged due to corrosion of steel plate with $FeCl_3$. At 1 M $FeCl_3$, the septum gets corroded and holes were observed on steel plate as shown in Fig.3.20.

The durability of the cell with concentration of $FeCl_3$ is shown Fig.3.21.

Another cell showed V_{OC} = 0.722 volts and I_{SC} = 85 mA after charging in 60 minute. For this cell after 20 hours it was observed that at two, three points on the steel plate, blackish solid like drops appeared into the first compartment. This means steel plate corrode due to high

Fig.3.20. Photograph of corroded septum cell.

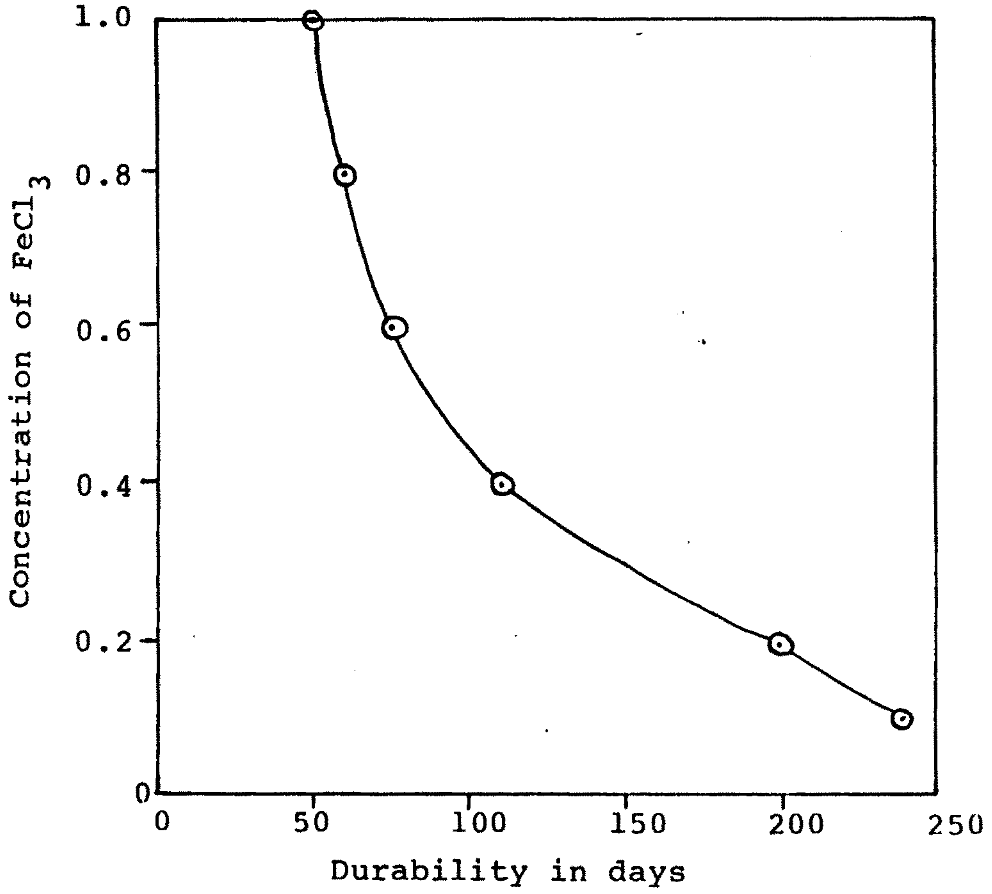

Fig.3.21. Durability of semiconductor seputm with concentration.

concentration of $FeCl_3$. The corrosion was not uniform but appeared at particular points.

In another cell we have used 0.1 M $FeCl_3$, then after one hour charging, it was observed that V_{OC} = 0.594 volts and I_{sc} = 23 mA. Thus as the concentration of $FeCl_3$ decreases, the current also decreases. The variation of I_{sc} with time is shown in Fig.3.22.

The power extracted from the cell is more for the cell with 1 M $FeCl_3$ and it decreases with decrease in concentration of $FeCl_3$. However, it is found that as concentration increases, there starts the corrosion of semiconductor septum solar cell. At 1 M $FeCl_3$, the septum gets corroded and holes were observed on steel plate. This might be due to the fact that stainless steel contains Ni, Cr, Co and Fe, so when steel is in contact with $FeCl_3$, then there is a removal of Ni, Cr and Co from the steel and only Fe remains as it is so holes are created. If we use iron instead of steel then there might be no corrosion.

3.4 MODELLING OF SC-SEP SOLAR CELLS : RESULTS AND DISCUSSION

3.4.1 Priliminaries

The smallest active elements of photovoltaic generators are modules in which single solar cells are combined into one mechanical and electrical unit. Output voltage and output current are matched to demand through a

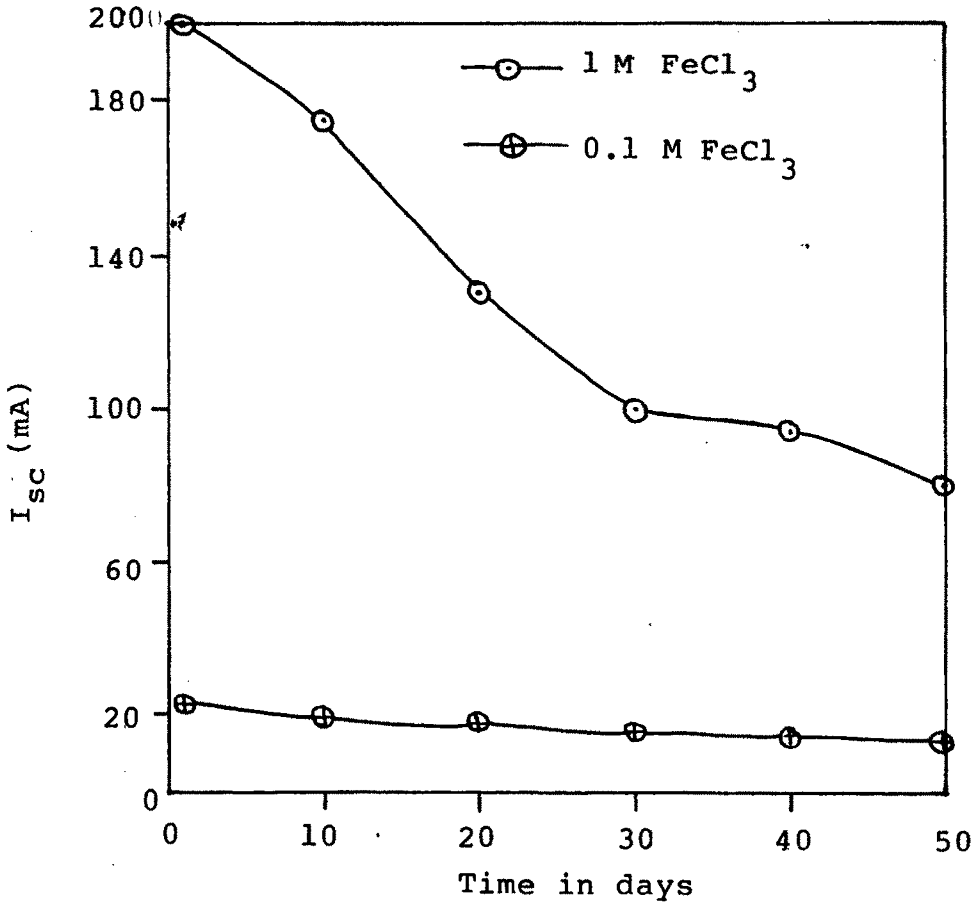

Fig.3.22. Variation of current with time.

combination of modules in series or parallel circuits. The number of modules determines the plant's capacity.

Analogous to modules, where individual cells are interconnected, the characteristic electrical features of photovoltaics are retained in the construction of larger generators. Solar generators, therefore, can also be characterized in terms of the short circuit current, no-load voltage, maximum power point (MMP) and the fill factor.

Generally, a large generator field is divided electrically into individual groups, each of which can deliver the required system voltage. These groups can e shut down separately in the event of malfunction and can be maintained without having to shut down the entire generator. Within each individual group there are many modules in series that are connected again in parallel circuits.

Even with optimum matching, the circuitry symmetry can be disturbed by degradation of individual cells, breakage, corrosion of leads or partial shadowing. Because such asymmetries lead in extreme cases to the destruction of the cell due to thermal overload ("hot spots"), protective diodes must be installed.

Bypass or shunt diodes prevent shadowed cells or those with low short-circuit currents in a serial circuit from being operated in reverse as consumers. They also ensure that only a small number of cells become ineffective and that the whole string doesn't fail because of a break in the serial circuit. Since the break-through voltage potential of solar cells operated in reverse direction is above 10 V but their open - circuit voltage is at most 0.6 volts, it is sufficient to combine 10 to 15 cells in series with one parallel diode.

Blocking diodes are switched between parallel strings. They protect a string with low output voltage from having to absorb current in reverse direction, reducing a group's total output voltage as internal load. In contrast to bypass diodes, blocking diodes conduct current in normal generator operation.

Here series combination, parallel combination and series-parallel combination of SC-SEP solar cells have been studied and explained in the following sections.

3.4.2 Series Combination of SC-SEP Cells

For number of electric devices, one needs different power supplies with certain voltages and current capacity. In order to get power supply and the desired voltage, one has to connect the primary unit cells in series. In view of this, we have studied, the series combination of semiconductor septum solar cells.

(a) When the two cells of semiconductor septum film area 100 cm^2 filled with 1 M polysulphide in compartment I and 1 M $FeCl_3$ in compartment II, were connected in series, then it was observed that V_{OC} = 1.73 volts and I_{sc} = 143 mA.

The light emitting diode (LED) when connected across the electrodes of these two cells, it gets enlighted.

This means that the current capacity of one cell is sufficient to operate light emitting diode.

(b) The variation of voltage and current with number of septum cells in series were studied.

The variation of voltage with 5 number of cells in series for different areas of semiconductor film and different concentration of $FeCl_3$ in compartment II is shown in Fig.3.23.

From Fig.3.23, it is seen that as number of cells is series increases, the voltage increases, which is in good agreement with theoretical concept. It is also seen that the cell voltage decreases as concentration of $FeCl_3$ decreases.

For the series combination the value of current nearly remains constant.

3.4.3 Parallel Combination of SC-SEP Cells

For getting higher current we have to connect the

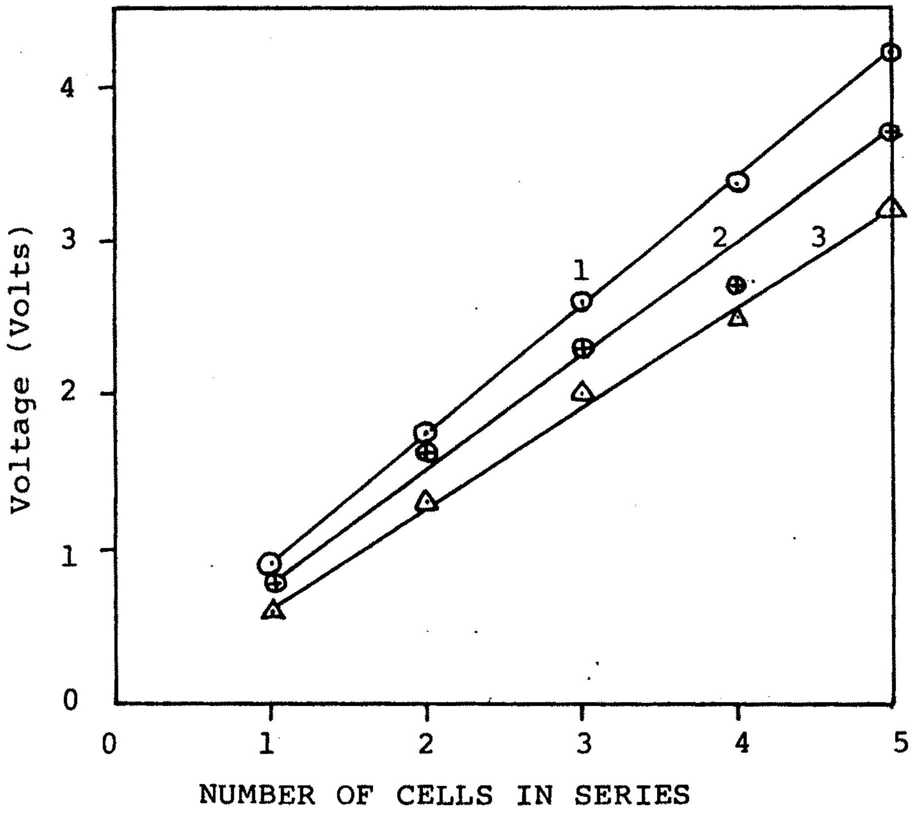

Fig.3.23. Variation of voltage for 5 no. of cells for
1. 1M $FeCl_3$ and area of film = 100 cm^2
2. 1M $FeCl_3$ and area of film = 80 cm^2
3. 0.1M $FeCl_3$ and area of film= 80 cm^2

number of cells in parallel. in view of this, we have studied, the parallel combination of semiconductor septum solar cells.

The variation of current with number of semiconductor septum solar cells in parallel for different areas of semiconductor film and different concentration of $FeCl_3$ in compartment II is shown in Fig.3.24.

From Fig.3.24, it is seen that as the number of cells in parallel increases, the current increases, which is in good agreement with theoretical concept. The value of the voltage nearly remains constant. So one can achieve the required current by connecting the number of cells in parallel.

It also seen that, for higher concentration of $FeCl_3$ in compartment II, the current is high, and for lower concentration, the current is low. This is mainly due to the fact that, the increase in concentration increases the number of Fe^{3+} ions and therefore, more number of electrons generated in the semiconductor septum are utilised to convert Fe^{3+} into Fe^{2+}.

3.4.4 Series - Parallel Combination of SC-SEP Solar Cells

From the idea of PV system, it is possible to connect the number of cells in series and parallel to meet

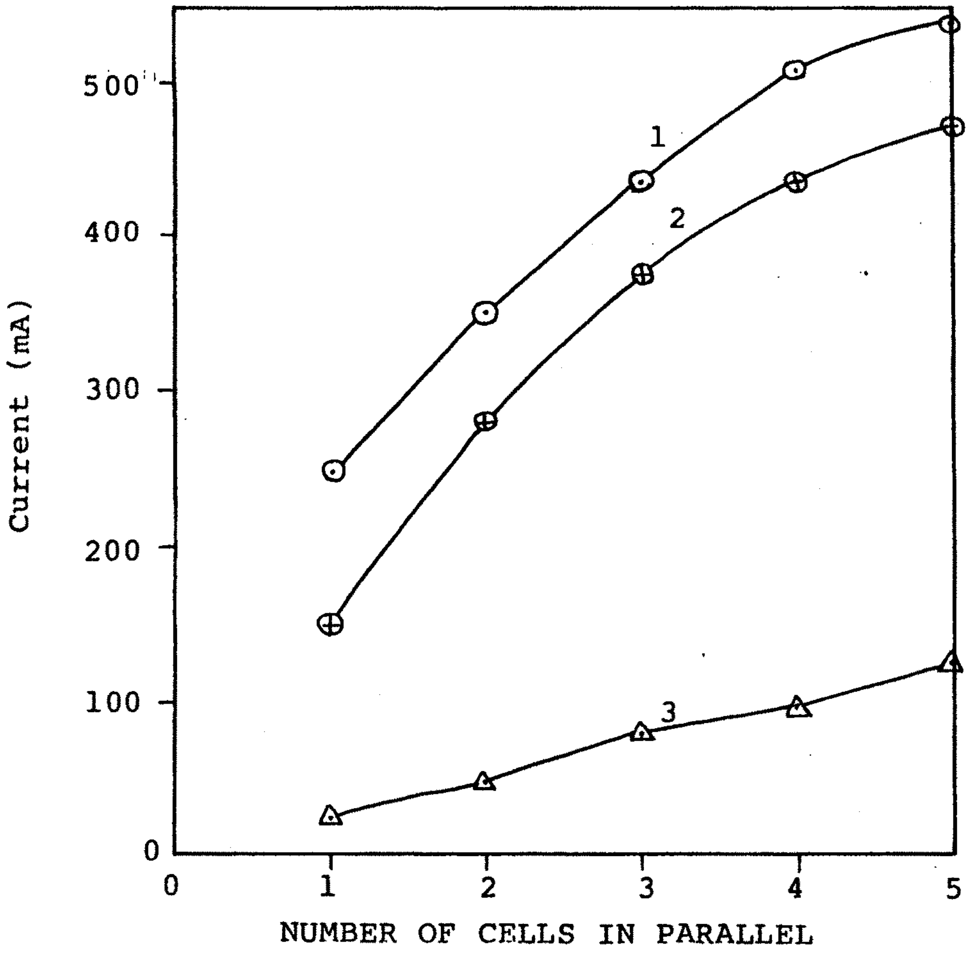

Fig.3.24. Variation of current for 5 no of cells for
1. 1M $FeCl_3$ and area of film = 100 cm^2
2. 1M $FeCl_3$ and area of film = 80 cm^2
3. 0.1 M $FeCl_3$ and area of film= 80 cm^2

the requirement and a desired power supply. We have studied the series - parallel combination of SC-SEP solar cells by different number of ways.

For example, the three semiconductor septum solar cells show separately the values of V_{OC} and I_{sc} as follows :

For cell 1, V_{OC} = 0.80 volts and I_{sc} = 100 mA
For cell 2, V_{OC} = 0.80 volts and I_{sc} = 110 mA
For cell 3, V_{OC} = 0.90 volts and I_{sc} = 90 mA

When these three cells were connected in series, then it was observed that

V_{OC} = 2.56 volts and I_{sc} = 80 mA

When these three cells were connected in parallel then it was observed that

V_{OC} = 0.797 volts and I_{sc} = 250 mA

When cells 1 and 2 were in parallel and cell 3 was in series with this, then it was observed that,

V_{OC} = 1.4 volts and I = 150 mA

We have studied the series - parallel combination for 6 number of cells. The series - parallel combination is shown in Fig.3.25.

When three cells were in series and another three cells in series and connecting these two combination in parallel, it was observed that

V_{OC} = 2.50 volts and I_{sc} = 280 mA.

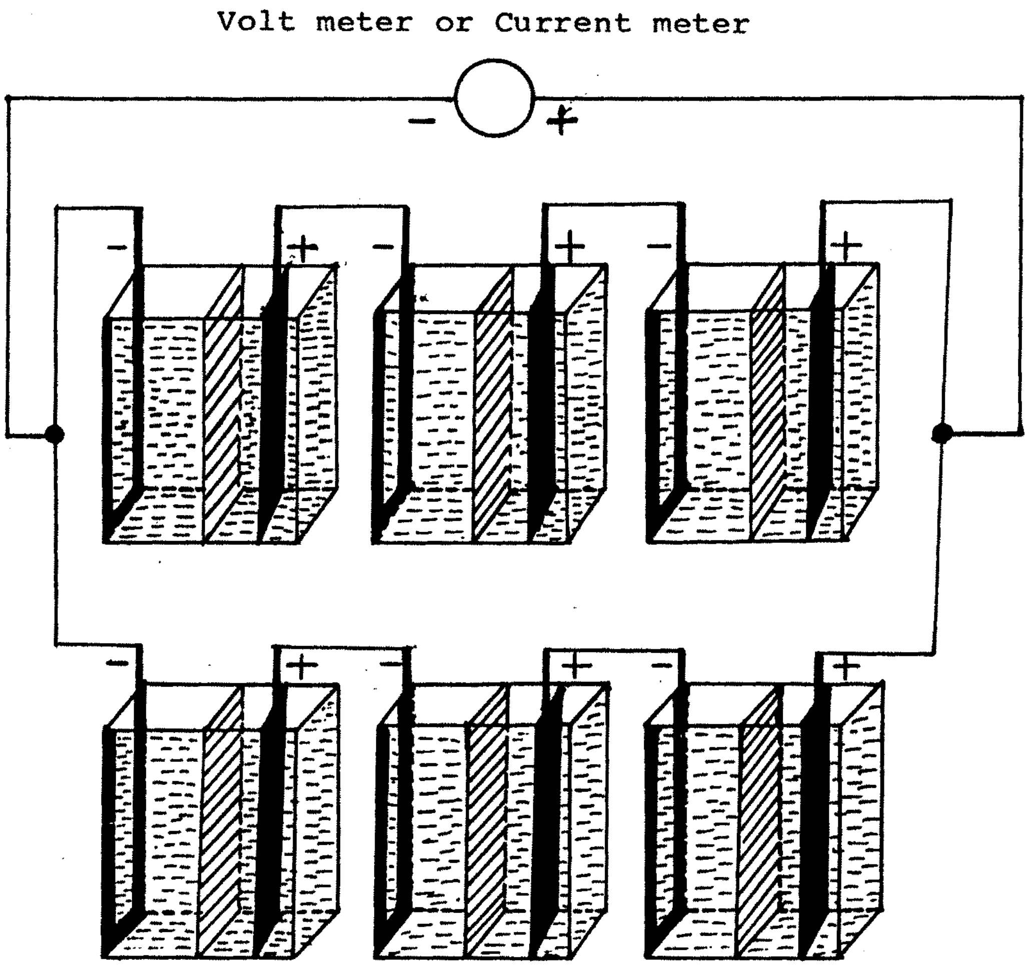

Fig.3.25. Schematic representation of series-parallel combination.

Fig.3.26. Photograph of 12 no. of cells prepared.

According to theoretical concept, it is expected that, if each cell gives voltage 1 volts and current 100 mA, then when these cells are connected in series, it should give voltage 3 volts and current 100 mA and when these cells are connected in parallel it should give voltage 1 volt and current 300 mA.

However, in our study it is not so. When the cells were connected in series or parallel or series - parallel combination, then it was observed that the results were less than the expected one. This may be due to the fact that, when the number of cells are connected in series - parallel combination, then there will be charge transfer reactions between the number of cells, internal losses of the cells which results in decrease in voltage and current.

By using number of semiconductor septum solar cells in series - parallel combination, one can obtain desired power supply.

3.5 CONCLUSION

Cadmium selenide (CdSe) films of area 80 cm^2 were deposited on stainless steel substrate by D.C. electrodeposition method having all parameters optimized. The same stainless steel was used as counter electrode. It was observed that the films were very much sticky and uniform as compared to the films obtained by graphite as counter electrode.

It is demonstrated that the solar energy can be stored in the form of chemical energy using n-CdSe semiconductor septum solar cells. When only compartment I was filled with polysulphide solution, then photovoltage and photocurrent were increased with increase in light intensity. Photocurrent also found to dpend upon the area of film. When graphite was used as counter electrode in PEC cell, then photocurrent was 6.5 mA and when stainless steel was used, then it was 0.52 mA. Thus stainless steel is not suitable for PEC cell as a counter electrode.

Semiconductor septum solar cells of different area of films were studied. For 100 cm^2 area of the film, one of the cells showed that I_{sc} = 300 mA and V_{oc} = 1.00 volts. For 80 cm^2 area of the film I_{sc} = 200 mA and V_{oc} = 1 volts. These are the values after charging the cell in 1 hour, with intensity of light 80 mW/cm^2. In compartment I, polysulphide solution of 1 M concentration was kept fixed and varying the concentration of $FeCl_3$ in compartment II was also studied. It was obsrved that for 1 M concentration of $FeCl_3$ I_{sc} = 200 mA and V_{oc} = 1 volts in one of the cells. In another cell it was observed that I_{sc} = 163 mA and V_{oc} = 0.822 volts. For 0.5 M concentration of $FeCl_3$, it was observed that V_{oc} = 0.7

volts and I_{sc} = 80 mA. For 0.1 M concentration, V_{oc} ≐ 0.6 volts and I_{sc} = 22 mA, after charging the cells in 1 hour, with intensity of light 80 mW/cm^2. Thus it is concluded that at high concentration, the current is large. The current capacity of the cell decreases with decrease in concentration of $FeCl_3$. This might be due to the fact that, the availability of number of Fe^{3+} ions for the reduction reaction in compartment II. The increase in concentration increases the number of Fe^{3+} ions and therefore more number of electrons generated in the semiconductor septum are utillised to convert Fe^{3+} into Fe^{2+}. Discharging characteristics were also studied. Continuous power could be generated through an external load more than 4 hours. The power extracted from the cell was more for the cell with 1 M $FeCl_3$ and it decreased with decreased in concentration of $FeCl_3$. However, it was found that as concentration increases, there starts the corrosion of semiconductor septum cell. At 1 M $FeCl_3$, the septum gets corroded and holes were observed on steel plate. So high concentration of $FeCl_3$ is not suitable for the cell.

The series combination of semiconductor septum solar cell was studied. When the two cells each having, 100 cm^2 area of the film and filled with 1 M polysulphide in compartment I and 1 M $FeCl_3$ in compartment II, it was observed that V_{OC} = 1.73 volts and I_{sc} = 143 mA. Light emitting diode (LED) was operated, with these two cells in series. When 5 cells were connected in series, it gives maximum voltage of the order of 4.2 volts, while parallel system gives maximum current of the order of 540 mA.

Six cells in series-parallel combination gives V_{OC} = 2.50 volts and I_{sc} = 280 mA. By using number of semiconductor septum solar cell in series and parallel combination one can obtain desired power supply.

REFERENCES

1. Gerischer, H. Electroanal. Chem. and Interface Electrochem. 58 (1975a) 263.
2. Sharon, M., Veluchamy, P.,Natarajan, C. and Kumar, D., Electrochemica Acta. 36 (1991) 1107.
3. Sharon, M. and Pandey, R.K., Phys. Stat. Sol(a), 52 (1982) 415.
4. Prasad, G., Chandra babu, K.S. and Shrivastava, O.N., Int. J. Hydrogen Energy 13 (1989).
5. SubbaRao, G.V., Aruchmy, A., Aravamudan, G. and Paranthama, M., Adv. Hyd. Energy, Prog. 3 (1984) 1075.
6. Manivanan, A., Aruchamy, A., Aravamidan, G. and SubbaRao, G.V., Solar Energy Mat. 15 (1987) 293.
7. Agarwal, M.K., Patel, H.B. and Reddi, K.N., J. Crystal Growth 41 (1977) 84.
8. Chandra, S. and Pandey, R.K., Phys. Stat. Sol. (a) 59 (1980) 787.
9. Mangalhara, J.P., Thangaraj, R. and Agnihotri, O.P., National Workshop on Energy Resources Through Photoelectrochemical Routes, Kolhapur. 5 (1987) 60.
10. Manassen, J., Hodes, G. and Cahen, D., J. Eelectrochem. Soc., 124 (1977) 532.
11. Hodes, G., Manassen, J. and Cahen, D., Nature, 102 (1976) 403.

12. Tien, H.T., Z-C Bi and Tripathy, A.K., Photochem. Photobiol. 44 (1986) 779.

13. Ottova, A., Otto, M. and Cerhata, D. Bull. of Electrochem. 7 (1991) 232.

14. Patil, P.S. and Pawar, S.H., J. Bull. Electrochem. 5 (1989) 618.

15. Pawar, S.H. and Patil, P.S., Bull. of Electrochem. 6 (1990) 618.

16. Pawar, S.H., Patil, M.P. and Shinde, V.N., Bull. of Electrochem. 9 (1993) 252.

17. Hardee, K.L. and Bard, A.J. Electrochem. Acta. 122 (1975) 739.

18. Hardee, K.L. and Bard, A.J. Eelectrochem. Acta. 123 (1976) 1024.

19. Hardee, K.L. and Bard, A.J., J. Electrochem. Soc. 124 (1977) 215.

20. Pawaskar, N.R., Menezes, C.A. and Sinha, A.P. B., J. Electrochem. Soc. 124 (1977) 743.

21. Chamberlin, R.R. and Skarman, J.S., J. Electrochem. Soc. 113 (1966) 86.

22. Subramanian, V., Murali, K.R., Rangarajan, N. and Lakshmanan, A.S. Bull. Mater. Sci., Vol.17, No.6 (1994) 1049.

23. Lokhande, C.D., Yermune, Y.S. and Pawar, S.H., J. Materials Chemistry and Physics, 20 (1988) 283.

24. Shanthi, E., Banergee, A., Dutta, V. and Chopra, K.L., Thin Solid Film 71 (1980) 237.

25. Menaseen, J., Hodes, G. and Cahen, D. in A Heller ed. Semiconductor Liquid Junction Solar Cells, Electrochem. Soc. Inc. Princeton (1977) 34.

26. Tien, H.Ti., Nature 227 (1970) 1232.

27. Chandra, S. and Pandey, R.K., Phys. Stat. Solidi (a) 59 (1980) 787.

28. Chandra, S. and Pandey, R.K., Stat. Solidi (a) 72 (1982) 415.

29. Chandra, S., Pandey, R.K. and Agarwal, R.C., Solar Cell, 1 (1980) 367.

30. Lokhande, C.D., Dabhade, R.V., Patil, P.S. and Pawar, S.H., Bull. of Electrochem. 7 (1991) 319.

31. Murali, K.R., Subramanian, V., Rangarajan, N., Nagaraja Rao, K. and Lakshmanan, A.S. Fourth International Conference on Frontiers of Electrochemistry, India (14-16) (1989).

32. Panicker, M.P.R. et al., J. Electrochem. Soc. 125 (1978) 566.

33. ASTM data card Nos. 8-461 and 8-459.

34. Pawar, S.H., Patil, M.P. and Shinde, V.N., Bull. Electrochem. 9 (1993) 252.

35. Studies on CdSe Semiconductor Septum Solar Cells, Ph.D. Thesis (1994) by M.P. Patil, Shivaji University, Kolhapur.

36. Pawar, S.H., Bhosale, C.H. and Patil, R.N., Solid State Energy Conversion, S.U. Kolhapur (1985) 28.

37. Gerischer, H. in 'Phys. Chem. An advanced treatise' Ed. Eyring H. Vol. IX A A.P. (1970) 463.

38. Gerischer, H. in 'advanced in Electrochem. L. Electrochem. Engg. Vol. 1 Ed. Delahay P.I.P. New York (1961) 193.

39. Freund, T. and Gomes, W.P., Catal. Rev. 3 (1969) 1.

40. Green, M. in Modern Aspects of Electrochem. Ed. Bockris J O'M Vol. 2 LONDON (1959) 343.

41. Myamlin, V.A. and Pleskov, Y.V., Electrochem. of Semicond. Plenum Press, N.Y. (1967).

42. Dewald, J.F., in Semiconductors Acs, Monograph No. 140, Ed. N.B. Hanny, Reinhold New York (1959).

43. Dewald, J.F., in Surface Chem. of Metals and Semiconductors Ed. Gatos, H.C. New York (1960).

44. Brattain, W.H. and Garrett, G.B. Ann. New York Acad. Sci. 58 (1954) 951.

45. Brattain, W.H. and Garrett, G.B. Bell. Syst. Tech. J. 32 (1955b) 1.

46. Myamlin, V.A. and Pleskov, Y.U. V. Electrochemistry of Semiconductors (Academic Press, New York) (1967).

47. Vijh, A.K. Electrochemistry of Metals and Semiconductors (Marcel Dekker New York) (1973).

48. Gerischer, H. In Physical Chemistry - An Advanced Treatise, ed. H. Eyring, D. Henderson and W. Jost, Vol. IX A, (Academic Press, New York) (1970).

49. Gary Hodes, Joast Manassen and David Cahen, J. Electrochem. Soc. (1981) 2325.

50. Mishra, S., Tiwari, S. and Chardra, B.P., Bull. Mater. Sci., Vol. 17, No. 4 (1994) 429.